Investigating the Importance of RAB7 in C2C12 Myoblast Differentiation

by

James Patrick Thoms

A thesis
presented to the University of Waterloo
in fulfillment of the
thesis requirement for the degree of
Master of Science
in
Kinesiology

Waterloo, Ontario, Canada, 2021

Author's Declaration

I hereby declare that I am the sole author of this thesis. This is a true copy of the thesis, including any required final revisions, as accepted by my examiners.

I understand that my thesis may be made electronically available to the public.

Abstract

Prior research has shown that autophagy and mitophagy are intimately linked to skeletal muscle differentiation and myogenesis. Recent studies show that the RAB7 cycle is crucial in multiple stages of autophagy and mitophagy; however, few studies examine the importance of RAB7 in muscle physiology. The objective of this study was to explore the significance of RAB7 in mammalian myoblast differentiation and myogenesis. The protein expression and localization patterns of 4 constituents of the RAB7 cycle (RAB5, CCZ1, RAB7, and RABGDI) were characterized over 5 days of differentiation. These experiments showed two major findings. Differentiation of C2C12 cells induced changes in protein content and localization of RAB5, CCZ1, RAB7, and RABGDI, meaning that differentiation and the RAB7 cycle are linked. Furthermore, RAB7 mostly localizes to mitochondrial-enriched fractions, suggesting that RAB7 is highly active and participates in mitochondria dynamics. Next, differentiating C2C12 cells were transfected with RAB7 siRNA or chronically treated with CID1067700. These experiments show three notable findings. RAB7 inhibition results in negligible changes to RAB5, CCZ1, and RABGDI content suggesting there is a compensatory RAB7-independent mechanism. Differentiation and myogenesis are affected by RAB7 inhibition as observed by dramatic decreases in MYH content and various morphological measures. These differentiation deficits were likely caused by defective autophagy and ubiquitin proteasome system (UPS), as given evidence by accumulating LC3-II, unstable SQSTM1, decreased proteasome activity, and potentially lessened autophagic flux. Overall, this is the first study to show that RAB7 is critical to mammalian myoblast differentiation and myogenesis, and that RAB7-mediated defects in differentiation are likely caused by faulty autophagy, the UPS, and the crosstalk between them.

Acknowledgements

First and foremost, I would like to thank my supervisor, Dr. Joe Quadrilatero, for his enduring support and guidance throughout my thesis. I am excited to continue working with you in the future. I am grateful to my committee members, Dr. Robin Duncan and Dr. Dale Martin, for providing valuable insight and helpful feedback on my work. To my fellow MBCD lab-mates, thank you for your assistance both in and out of the lab. I appreciate the continual support of my friends and family throughout the completion of this project. To my partner, thank you for being my dependable editor, critic, and source of encouragement. Thank you to the University of Waterloo Faculty of Health and the Natural Sciences and Engineering Research Council of Canada. My research would not be possible without their financial support.

Table of Contents

List of Figures

List of Abbreviations

ALR, autophagic lysosome reformation

ALF, autophagosome-lysosome fusion

ATG, autophagy related

BECN1, beclin 1, autophagy related

BNIP3, BCL2/adenovirus E1B interacting protein 3

CCZ1, CCZ1 vacuolar protein trafficking and biogenesis associated

CF, cytosolic-enriched fraction

CID, CID1067700

CMT2B, Charcot-Marie-Tooth disease type 2B

CTRL, control

CQ, chloroquine

CuZnSOD/SOD1, superoxide dismutase 1, soluble

D, day of differentiation

DM, differentiation media

DNM1L/DRP1, dynamin-1-like

FIS1, fission, mitochondrial 1

GAP, GTPase activation proteins

GDI, GDP dissociation inhibitors

GDP, guanosine diphosphate

GEF, guanine nucleotide exchange factors

GM, growth media

GTP, guanosine triphosphate

LAMP, lysosome-associated membrane protein

MAP1LC3/LC3, microtubule-associated protein light chain 3

MF, mitochondrial-enriched fraction

MnSOD/SOD2, superoxide dismutase 2, mitochondrial

MON1, MON1 homolog, secretory trafficking associated

MYH, myosin heavy chain

MYOG, myogenin

OMM, outer mitochondrial membrane

PI3K, phosphoinositide 3-kinase

PI3P, phosphatidylinositol 3-phosphate

PINK1, PTEN induced putative kinase 1

PPARGC1A/PGC1α, peroxisome proliferative activated receptor, gamma, coactivator 1 alpha

PRKN, parkin RBR E3 ubiquitin protein ligase

RAB, member RAS oncogene family

siRAB7, RAB7 knockdown

RABGEF1, RAB guanine exchange factor 1

RUBCN, RUN domain and cysteine-rich domain containing, Beclin 1-interacting protein

Scr, scramble control

SQSTM1, sequestosome 1

STX17, syntaxin 17

TBC1D, Tre2/Bub2/Cdc16 1 domain family

TGFβ, transforming growth factor, beta

Ub, ubiquitin

UPS, ubiquitin-proteosome system

Vps34/PIK3C3, phosphatidylinositol 3-kinase catalytic subunit type

Chapter 1: Introduction and RAB7 Literature Review

1.1 Introduction

Skeletal muscle is a dynamic tissue that adapts and repairs throughout the lifespan. Muscle stem cells called satellite cells are able to replicate and undergo cellular differentiation, which aids in muscle tissue repair and growth (1). Differentiation results in cell specialization through altered gene and protein expression, ultimately changing cell function and morphology (2). After a stimulus such as mechanical injury or exercise, quiescent satellite cells become activated and start to proliferate (3-5). Some satellite cells replenish the satellite cell pool, while others become proliferative myoblasts (3,4). Some myoblasts fuse together to generate new myofibres through myogenesis, while others fuse to pre-existing myofibres (4,6,7). Mononuclear satellite cell differentiation is critical in muscle repair and growth (4,6,7). Myoblast differentiation and myogenesis are complex cellular processes associated with rapidly increasing myosin (MYH) content, increased number of multinucleated myofibres, and fluctuating myogenin (MYOG) content (4,6,7). There is a substantial amount of biosynthesis during myoblast differentiation; however, recent literature shows that it is also accompanied by extensive degradation (8-13). Thus, recent studies are shifting focus toward uncovering the role of autophagy, the predominant cellular degradation pathway, in muscle differentiation and myogenesis.

1.2 Autophagy

Autophagy is a collection of continuous cellular processes that promote cell survival by degrading unused and damaged cytosolic content, including proteins and organelles (10,14,15). There are three main types of autophagy: macroautophagy, microautophagy, and chaperone-mediated autophagy (14,15). During macroautophagy, membranal organelles called

autophagosomes sequester and transport ubiquitin (Ub)-tagged cytosolic cargo (14,15). Autophagosomal cargo is then degraded once autophagosomes fuse with hydrolase-filled lysosomes (14,15). Microautophagy utilizes pre-existing endosomes and lysosomes to directly sequester cytosolic content through membranal invaginations (14,15). Chaperone-mediated autophagy relies on chaperone proteins identifying specific chemical motifs and transporting these selectively targeted substrates across the lysosomal membrane (14,15). Since this thesis focuses solely on macroautophagy, it will henceforth be referred to as autophagy.

Autophagy is activated by various stressors including starvation, oxidative stress, DNA damage, and hypoxia (14,16-18). Once a pro-autophagy signal is detected, the ULK1 (Unc-51-like kinase 1) initiation, PI3P (phosphatidylinositol 3-phosphate)-binding, and PI3K III (phosphoinositide 3-kinase) nucleation complexes promote the formation of a lipid membrane termed a phagophore (14,15). Although the PI3K III complex promotes autophagy, two core proteins in this complex, BECN1 (Beclin 1, autophagy related) and Vps34/PIK3C3 (phosphatidylinositol 3-kinase catalytic subunit type 3), interact with RUBCN (RUN domain and cysteine-rich domain containing, Beclin 1-interacting protein) which is a potent autophagy inhibitor (14,15,19, 20). Once the phagophore is generated, it is expanded with MAP1LC3/LC3 (microtubule-associated protein light chain 3) and various ATG proteins such as ATG7 (autophagy related 7) and ATG9 (autophagy related 9) (14,15). A mature autophagosome is an LC3-II positive membrane that adequately surrounds SQSTM1 (sequestosome 1)-tagged cytosolic content that are ubiquitinated (14,15,21,22). Fully developed autophagosomes are transported by attaching to microtubule motors such as Kinesin or Dynein, for anterograde or retrograde transport, respectively (23). Autophagosomes then fuse to LAMP (lysosome-

associated membrane protein)-positive hydrolase-filled lysosomes to create autolysosomes (24). Autolysosomal hydrolases degrade sequestered content so that new structures can be built to reduce cellular stress (25-27). Once autolysosomes degrade their contents, autophagic lysosome reformation (ALR) initiates (28). ALR is a negative-feedback loop that reuses components of autolysosomes to regenerate new lysosomes through autolysosome membrane budding, tubulation, and proto-lysosome scission (28). Overall, autophagy is critical to cellular health, as shown in various mouse *Atg* knockout models resulting in fatal developmental complications (reviewed in 29). Notably, autophagy and another major intercellular degradation pathway, the UPS (ubiquitin-proteosome system), create a compensatory balance when either are compromised (30). In brief, the UPS involves protein complexes called proteasomes which breaks down Ub-tagged proteins through proteolysis (30).

Recent literature has begun investigating the connection between autophagy and myoblast differentiation. As indicated by increases in LC3-II, rapid depletion of SQSTM1, and significant accumulation of both proteins after chloroquine (CQ) treatment, myoblasts experience an autophagic flux as early as 12-hours after the induction of differentiation (11-13,29). Multiple parts of the autophagy pathway are crucial for C2C12 murine myoblast differentiation, including autophagosome biogenesis, autophagosome-lysosome fusion (ALF), and lysosome acidification. For example, chemical inhibition of autophagy using 3-methyladenine (a PI3K inhibitor), bafilomycin (an ALF and lysosome acidification inhibitor), or chloroquine (an ALF inhibitor) results in in hindered C2C12 differentiation (10,12,31). Additionally, knockdown of *Atg7*, *Lamp1*, or *Lamp2* in C2C12 cells lead to deficits in myotube development and hypertrophy, with *Atg7* knockdown having the severest outcomes (13,29,32).

Altogether, these knockdown experiments show that autophagy is critical for myoblast differentiation. Recently, studies focusing on multiple members from the family of RAB (member RAS oncogene family) proteins show that RABs regulate several steps along the autophagy pathway (33).

1.3 The RAB7 Cycle

The RAB family of GTPases are highly conserved proteins expressed throughout many different tissues and species (34,35). RAB proteins play a variety of crucial roles in cells, the predominant function being vesicle trafficking (summarized in 34). RABs undergo cycles of activation (GTP-bound) and inactivation (GDP-bound) as facilitated by GEFs (guanine nucleotide exchange factors) and GAPs (GTPase activation proteins), respectively (36). RABs are deactivated by GTP hydrolysis, whereas activation is completed through GDP nucleotide exchange with GTP (36). GDIs (GDP dissociation inhibitors) assist in the transportation of inactive (GDP-bound) RAB proteins in the cytosol (36). This process of activation, deactivation, and transportation is termed the RAB cycle.

RAB7A (member RAS oncogene family 7A) is one member of the RAB family of proteins that plays an extensive role in maintaining cellular functionality and survival (37,38). For example, *Rab7A* knockout mice endure fatal complications during early embryonic development (39,40). Two RAB7 proteins exist: RAB7A and RAB7B; the latter was renamed RAB42 (38,41,42). These proteins are homologues rather than isoforms as they do not share critical motifs, exist on separate chromosomes, and share only 50% of their identity (38,41,42). Most studies focus on RAB7A, as its role is broader and more important for multiple cellular

processes. Thus, moving forward, RAB7A will be referred to as RAB7. RAB7 contains two "switch" regions (43,44). Both switch regions are responsible for controlling guanine nucleotide exchange, while the "switch-II" region also affects RAB7 activity through post-translational modifications (43,44). Specifically, the switch-II region contains a serine phosphorylation site (S72) that controls RAB7 localization (44). Some other RAB7 modifications include phosphorylation, dephosphorylation, ubiquitination, SUMOylation, and palmitoylation at various RAB7 residues that control RAB7 activity, localization, and guanine nucleotide exchange (43-45). Previous studies have shown that RAB7, its post-translational modifications, and the RAB7 cycle are important for endocytosis, microautophagy, apoptosis, xenophagy, tumour suppression, and membrane trafficking (summarized in 38).

The RAB7 cycle (**Figure 1**) is conserved between multiple cellular processes including autophagy, endocytosis, and mitophagy (43,46,47). This cycle is initiated by a protein called

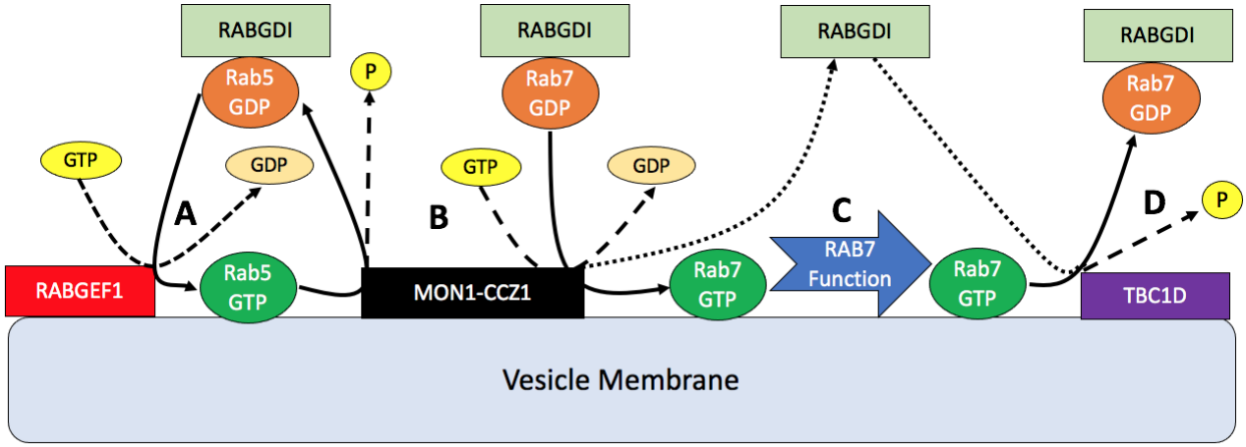

Figure 1: The RAB7 Cycle

(**A**) RABGEF1 adheres to a vesicle membrane and acts as a RAB5 GEF. (**B**) The MON1-CCZ1 complex is recruited by RAB5, and acts as a RAB5 GAP and a RAB7 GEF. (**C**) RAB7 performs its context-specific function (E.g., vesicle trafficking). (**D**) Various TBC1D proteins act as RAB7 GAPs to deactivate RAB7. RABGDI transports inactive RABs to and from the cytosol and the vesicle membrane.

RABGEF1 (RAB guanine exchange factor 1) that recruits and activates RAB5 (from RAB5-GDP to RAB5-GTP) which then adheres to early endosomes/autophagosomes (43,47; **Figure 1A**). RAB5-GTP recruits the MON1-CCZ1 (MON1 homolog, secretory trafficking associated-CCZ1 vacuolar protein trafficking and biogenesis associated) complex that displaces RABGEF1 and binds to PI3P (43,47; **Figure 1B**). This complex acts as a RAB5 GAP and a RAB7 GEF (43,47). Thus, MON1-CCZ1 facilitates RAB5 deactivation (RAB5-GTP to RAB5-GDP), while recruiting, activating, and adhering RAB7 (RAB7-GDP to RAB7-GTP) to the endosome/autophagosome membrane by interacting with RAB7's switch-II region (43,47; **Figure 1B**). While the exact mechanism of MON1-CCZ1 dissociation from the membrane is unknown, the top hypotheses are MON1-CCZ1 phosphorylation or PI3P hydrolysis (43,47; **Figure 1C**). During and after MON1-CCZ1 dissociation, RAB7 performs its context specific function (43,47; **Figure 1C**). Once RAB7's function is complete, a variety of RAB7 GAPs from the family of TBC1D (Tre2/Bub2/Cdc16 1 domain family) proteins deactivates (RAB7-GTP to RAB7-GDP) and facilitates RAB7 dissociation from the membrane (43; **Figure 1D**). Throughout the RAB7 cycle, the transport of both RAB5-GDP and RAB7-GDP to and from the membrane are mediated by RABGDI (43,47; **Figure 1A-D**). The RAB7 cycle regulates multiple stages of autophagy including autophagosome biogenesis, trafficking, autolysosome formation, and ALR as seen in **Figure 2** (33,37,38).

1.4 The RAB7 Cycle and Autophagy

RAB5 and RAB7 interact separately with the BECN1 and Vps34 subunits of the PI3K III nucleation complex to alter autophagy (48,49). RAB5 activates Vps34, leading to increased

autophagosome formation (48; **Figure 2A**). When RAB5 is inhibited, autophagosomal precursors such as ATG5 and ATG5-ATG12 conjugate accumulate in cells, whereas LC3-II is decreased (48). RAB7 facilitates the biogenesis and development of autophagosome-like vacuoles during GAS (Group A Streptococcus) xenophagy and autophagosomes during mitophagy in HeLa cells (49-51; **Figure 2A**). Although, it is unknown if RAB7 participates in autophagosome biogenesis during autophagy, there is some evidence to suggest that it does. For example, RUBCN interacts with both BECN1 and RAB7-GTP (52). RUBCN inhibits autophagy when bound to RAB7-GTP, but when RUBCN is absent or when the RAB7-GTP binding domain is faulty, autophagy is upregulated (52). Similarly, Vps34 regulates RAB7 activity by recruiting a RAB7 GAP called TBC1D2 during endocytosis (53). In sum, the interplay between autophagosome biogenesis factors Vps34 and BECN1, with RUBCN and RAB7 could suggest a potential upstream mechanism that links RAB7 to autophagosome formation. Once the phagophore develops into an autophagosome (**Figure 2B**), RAB7 then facilitates the transport of membranal structures such as endosomes and autophagosomes (33,38; **Figure 2C**). RAB7 transports membranal structures through interacting with FYCO1 (FYVE and coiled-coil domain containing 1) or RILP (RAB interacting lysosomal protein) and generating complexes with microtubule motors Kinesin and Dynein, respectively (33,38). Expression of the dominant negative form of RAB7 (T22N) impedes RILP's association with phagosomes, leading to a substantial decrease in phagosome-lysosome fusion when compared to the control (54). Next, RAB7 facilitates both endosome-lysosome fusion and ALF (38; **Figure 2C**). The PI3K complex binds to UVRAG (UV radiation resistance associated gene) and RAB7, in which the prior recruits the HOPS (Homotypic fusion and protein sorting) complex, ultimately leading to ALF

(55). RUBCN competes with RAB7-GTP for UVRAG binding to inhibit this process (56). However, it is still under debate whether this RAB7-dependent ALF mechanism applies to mammalian cell biology (57; **Figure 2C**). For example, some evidence shows that RAB7 may be dispensable from ALF in some mammalian cell types during glutamine starvation (57). Finally, RAB7 also regulates ALR, the process by which lysosomes are regenerated from autolysosomes (58; **Figure 2D**). One study found that RAB7 must dissociate from the autolysosomal membrane before ALR can occur (58).

Together, these RAB7-dependent mechanisms explain the autophagic deficits such as autophagosome/autolysosome accumulation seen in *Rab7* mammalian knockout and dominant negative models (57,59-61). Likewise, knockouts and dominant negative experiments of RAB7

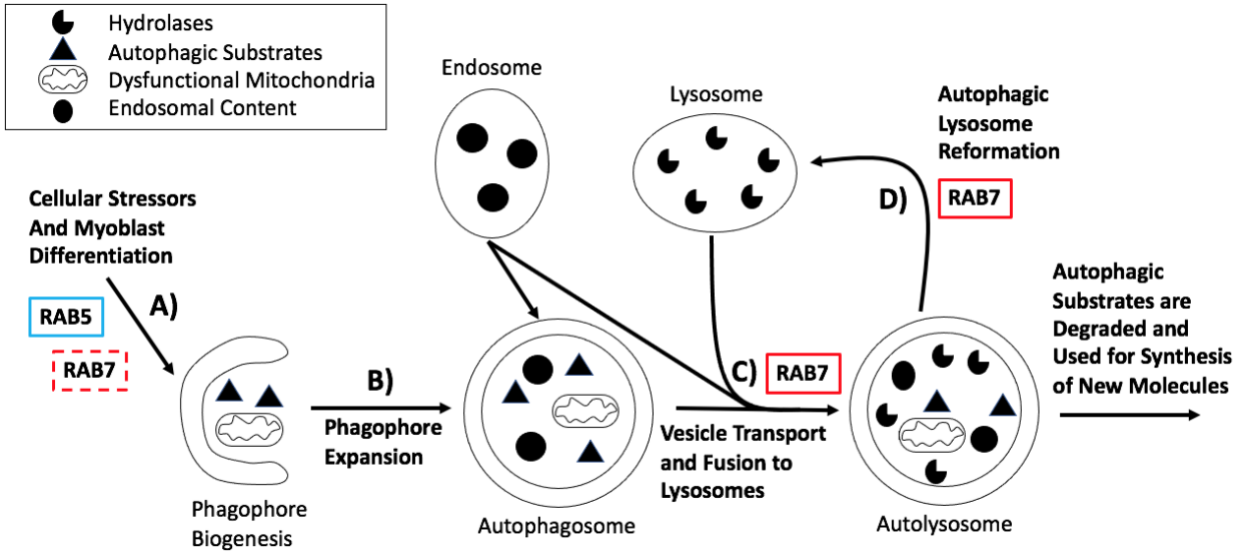

Figure 2: The Roles of RAB5 and RAB7 Along the Autophagy Pathway

(**A**) RAB5 (and possibly RAB7) mediates phagophore biogenesis. (**B**) The phagophore expands into a mature LC3-II positive autophagosome. (**C**) RAB7 facilitates vesicle transport (autophagosomes, endosomes, and lysosomes) as well as the fusion of endosomes and autophagosomes with lysosomes. (**D**) RAB7 also plays a role in ALR.

GAPs (TBC1D2, 5, and 15) result in autophagosome accumulation and reduced autophagosome formation (summarized in 43), while treatment with GTPγS (a non-hydrolysable form of GTP) led to hindered ALR (58). These findings provide strong evidence that not only is the presence of RAB7 important, but also its ability to participate in the RAB7 cycle by going through phases of activation and deactivation.

Previous literature has shown that RAB7 recruits and interacts with proteasome subunit alpha 7 (XAPC7/PSMA7) during late endocytosis (62). Furthermore, E3-Ub-ligase ring finger protein 115 (RABRING7/RNF115) interacts with and is recruited by RAB7 during late endocytosis, endosomal/lysosomal trafficking, lysosome biogenesis, and lysosomal acidification (63,64). When comparing the constitutively inactive dominant negative (T22N) and wild-type forms of RAB7, the interaction between RAB7 and PSMA7 or RNF115 was decreased in the T22N condition (62,64). Together, these studies connect RAB7 and its activity level to the UPS in two ways. RAB7 can influence proteasome (or at least PSMA7) activity and localization (62), and RAB7 mediates ubiquitination in specific circumstances (63,64). Since autophagy and the UPS use Ub tags to recognize targets (summarized in 30), RAB7 could influence both pathways through a common mechanism.

Mutations in the RAB7 gene that prevent RAB7 from participating efficiently in its cycle leads to a peripheral neuropathy disorder called CMT2B (Charcot-Marie-Tooth disease type 2B) (65). Symptoms of this disease, such as distal muscle weakness and atrophy, are believed to be caused by a lack of autophagy in neurons leading to neurodegeneration (65). Currently, there are no studies identifying if the mutated RAB7 gene causes autophagic deficits within skeletal muscle in CMT2B patients. Furthermore, it is unknown whether RAB7-dependent autophagic

deficits exacerbate distal muscle weakness and atrophy by impeding myoblast differentiation, fusion, and hypertrophy. Ultimately, because RAB7 performs multiple roles relating to autophagy, it is crucial to organismal and cell functionality. Recent studies have shown that RAB7 also facilitates mitophagy, the mitochondrial-specific form of autophagy.

1.5 Mitochondria and Mitophagy

Mitochondria are double-membraned organelles crucial to maintaining cellular health and performing critical functions such as energy creation, apoptosis, and cell signaling (66). Mitochondria are dynamic structures that can combine or excise portions of their complex networks through fusion and fission, respectively (66-68). An indicator of mitochondrial health is the maintenance of a chemiosmotic gradient between the mitochondrial matrix and the proton-filled intermembrane space (69). To maintain this potential, mitochondria fuse together and generate networks to rescue the function of damaged mitochondria (66,67). If the mitochondrial demands are greater than production, new mitochondria are synthesized through a PPARGC1A/PGC1α (peroxisome proliferative activated receptor, gamma, coactivator 1 alpha)-mediated process called mitochondrial biogenesis (67). Conversely, decreased proton gradient potential hinders mitochondrial function and can promote mitochondrial fission through increased expression of DNM1L/DRP1 (dynamin-1-like) (66,67). When a portion of an excised mitochondrion becomes dysfunctional, it will undergo mitophagy (67). Mitophagy can be activated by a variety of stimuli including decreased membrane potential, hypoxia, and oxidative stress (67,70). Mitochondrial dynamics and mitophagy are imperative for cellular health. One of

the most extensively researched mitophagy mechanism is the PINK1-PRKN (PTEN induced putative kinase 1-Parkin RBR E3 ubiquitin protein ligase) pathway.

PINK1 is a mitochondrial protein kinase that associates with the OMM (outer mitochondrial membrane) through TOMM (translocase of outer mitochondrial membrane) proteins (71). In healthy mitochondria, PINK1 is degraded by proteases once it passes through the OMM (71). However, PINK1 remains associated with the OMM once a mitochondrion becomes dysfunctional (71). This accumulation results in the recruitment of E3-Ub ligase PRKN (72). PRKN post-translationally modifies OMM proteins by adding Ub chains (71,72). This initiates the mitophagy program, leading to the recruitment of autophagic factors such as SQSTM1 and subsequently LC3-II (71). Employment of SQSTM1 and LC3-II results in the creation of a phagophore and its subsequent expansion as seen in the autophagy pathway (71; **Figure 2A-B**). Although the PINK1-PRKN pathway is the predominant form of mitophagy, other pathways have been identified. For example, other E3-Ub ligases such as MUL1 (mitochondrial ubiquitin ligase activator of NFKB) or MARCHF5 (membrane associated ring-CH-type finger 5), act in parallel to PRKN's post-translational modification function to promote mitophagy (73-75). MUL1 can even compensate for loss of PINK1/PRKN function in *Drosophila* and mammalian cells (75). Furthermore, LC3/GABARAP (gamma-aminobutyric acid receptor associated protein)-interacting proteins such as BNIP3 (BCL2/adenovirus E1B interacting protein 3) are responsible for the direct sequestration of mitochondria by attaching to the OMM and the autophagosome (73,74). Altogether, the proper balancing of mitochondrial fusion and biogenesis with fission and mitophagy is vital to mitochondrial function. Maintenance of mitochondrial function through mitochondrial dynamics is crucial to myoblast differentiation.

After the induction of differentiation, mitochondrial remodeling proteins DNM1L, OPA1 (OPA1, mitochondrial dynamin like GTPase), and PPARGC1A increase (10,13). There is fluctuating mitochondrial turnover during differentiation, favoring mitophagy during early differentiation and biogenesis during late differentiation (10,13). Since PRKN is absent in C2C12 cells, other pathways are mediated by BNIP3 and other E3-Ub ligases maintain mitochondrial clearance (13,73-75). BNIP3 protein expression and SQSTM1-mitochondrial localization are elevated during the first three days of differentiation (D1-3), the prior remaining elevated until D5 (10,13). This BNIP3 data, in addition to Yamada, et al. 2019 showing that SQSTM1 promotes ubiquitination of OMM proteins independently of PINK1 or PRKN, suggest that multiple alternative mitophagy pathways could be used during C2C12 differentiation (10,13,76). In *Bnip3* knockouts, *Atg7* knockdown, and bafilomycin-treated C2C12 cells, both mitophagy and differentiation are impaired (10,13). These experiments resulted in mitochondrial remodeling disruption, altered mitochondrial dynamics protein expression (PPARGC1A, DNM1L, and OPA1) and hindered expression of C2C12 differentiation markers MYOG and MYH (10,13). Altogether, this data supports that mitophagy is a crucial precursor in regulating mitochondrial remodeling and C2C12 differentiation. Studies are starting to uncover the crucial role of RAB7 in regulating PRKN-dependent and independent mitophagy pathways.

1.6 RAB7 and Mitophagy

Figure 3A shows that, once Ub-tagged OMM proteins start to accumulate during the initial stages of PRKN-dependent mitophagy, the RAB7 cycle initiates (77). Ub-OMM proteins employ RABGEF1, which attaches to long Ub chains and facilitates RAB5 activation and adherence to

the OMM (77). The RAB7 cycle proceeds until RAB7 is phosphorylated by TBK1 (TANK-binding kinase 1) increasing the recruitment efficiency of ATG9 and LC3 positive vesicles (78). To ensure proper encapsulation of the mitochondrion, a TBC1D15-17 complex attaches to autophagosomal LC3/GABARAP proteins and to OMM protein FIS1 (fission, mitochondrial 1) (79). This FIS1-TBC1D-LC3/GABARAP complex deactivates and removes RAB7 from the OMM, preventing excessive autophagosome expansion (77). Notably, the RAB7 mitophagy mechanism is nearly identical to the maturation of autophagosomes and endosomes (59).

Genetic interference of RAB7 results in reduced mitochondrial elimination. For example, siRNA mediated knockdown of *Rab7* or mutation of its phosphorylation site ($RAB7^{S72A}$), reduced recruitment of ATG9-positive vesicles and hindered mitochondrial sequestration (77,78). Additionally, *Rab7* knockdown cells treated with mitophagy inducer valinomycin have decreased mitochondrial clearance (77). Other RAB7-related proteins are also critical in PRKN-dependent mitophagy since siRNA knockdowns of *Rabgef1*, *Mon1*, and *Ccz1* have significantly decreased RAB7 recruitment to the mitochondria and diminished mitochondrial clearance (77). Furthermore, loss of RAB7 GAP TBC1D15 leads to excessive ATG9 and LC3 accumulation around damaged mitochondria, as well as reduced mitochondrial fission and clearance (43,77,80). These knockdown experiments demonstrate the importance of RAB7 and the RAB7 cycle during PRKN-mediated mitophagy.

The RAB7 cycle is also crucial to PRKN-independent mitophagy. For example, in HeLa cells that have little to no endogenous PRKN (81), RAB7 is localized on mitochondria (43,77). Genetic interference of various RAB7 GAPs, including TBC1D5, TBC1D15, and/or TBC1D17, results in hyperactive RAB7, which hinders ATG9A trafficking and mitophagy (43,79).

Specifically, *Tbc1d5* knockouts in HeLa cells results in lysosomal accumulation of RAB7 and reduced mitochondrial clearance (43). Furthermore, a study by Hammerling, et al. (2017) provides evidence that RAB5 works with BNIP3 during mitophagy (82). Mechanistically, BNIP3 signals for the direct engulfment of dysfunctional mitochondria in endosomes through microautophagy (**Figure 3B**) (82). While RAB7 has not been found to directly interact with BNIP3, Hammerling, et al. 2017 hypothesizes that E3-Ub ligases other than PRKN could be used to promote RAB7-dependent mitophagy seen in **Figure 3A** (82).[1] Even if this hypothesis is

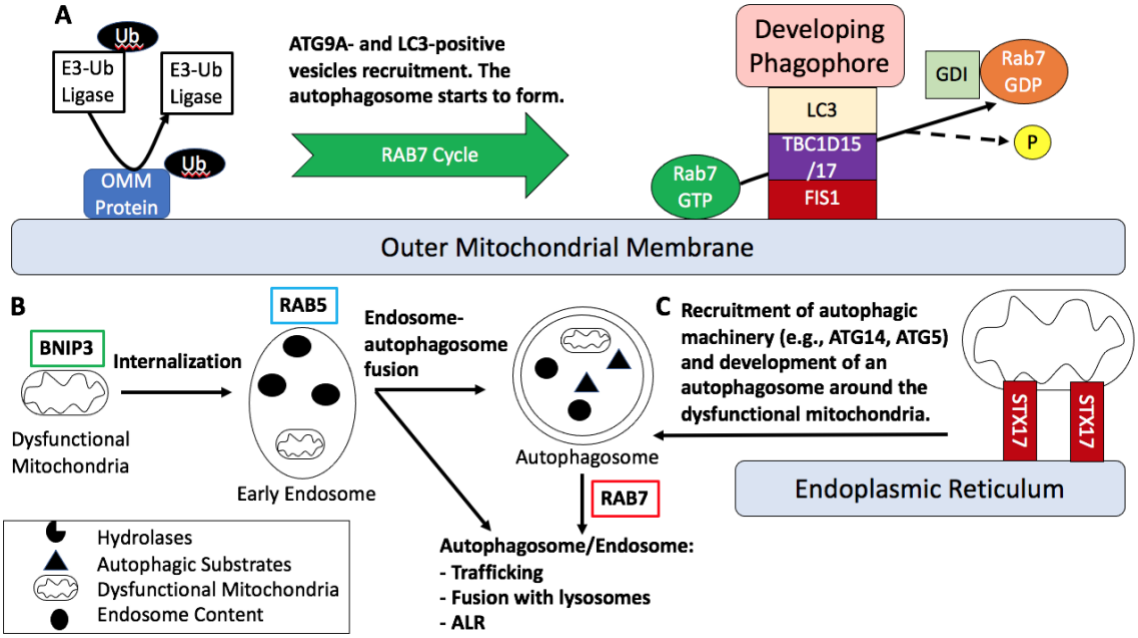

Figure 3: RAB7-Mediated Mechanisms of Mitophagy

(**A**) The PINK1-PRKN (or other potential compensatory E3-Ub ligases) pathway integrates the RAB7 cycle to generate phagophores around dysfunctional mitochondrion. (**B**) BNIP3-decorated mitochondria can be internalized into RAB5-positive endosomes through microautophagy. (**C**) Endoplasmic reticulum-bound STX17 facilitates autophagosome development (in *Fis1* knockouts) around dysfunctional mitochondria. Once the mitochondrion is sequestered, all three pathways converge on RAB7-dependent downstream autophagy mechanisms such as vesicle trafficking, fusion with lysosomes, and ALR.

[1] Hammerling, et al. 2017 specifically mentions MARCHF5, however they show no evidence that it is this specific E3-Ub ligase.

false, all currently known RAB5-dependent autophagy and mitophagy mechanisms converge to RAB7-dependent mechanisms (33; **Figure 3B**). Another study showed that both RAB7 and TBC1D15 are crucial to PRKN-independent STX17 (syntaxin 17)-dependent mitophagy (83; **Figure 3C**). *Fis1* knockout cells (a condition similar to C2C12 cells) that are also *Rab7* or *Tbc1d15* knockdowns result in drastically decreased autophagy protein recruitment such as ATG5 and ATG14 (83). These knockdown experiments hinder endoplasmic reticulum-bound STX17-mediated mitochondrial clearance (83).

Overall, RAB7 participates in multiple pathways critical to skeletal muscle including autophagy and mitophagy in various different cell types. However, few studies have explored the RAB7's role in muscle physiology, and even fewer explored its role in skeletal muscle physiology.

1.7 RAB7 and Skeletal Muscle Physiology

Currently, there are only three studies that explore the impact of RAB7 on skeletal muscle physiology. The first study by Nakamura, et al. (2014) implies that age-related decreases in endosomal RAB7 activity may lead to sarcopenia in aged rats (84). Nakamura et al.'s 2014 study is significant because it is the first to investigate the role of RAB7 in mammalian skeletal muscle physiology (84). However, this study did not directly connect RAB7 to sarcopenia, mention myoblast differentiation or fusion, or focus on any pathways other than endocytosis (84). Next, the study by Fujita, et al. (2017) found that *Rab7* knockdown results in autophagosome accumulation and disorganized T-tubule networks in Drosophila internal oblique muscles (85). Despite Fujita, et al. (2017)'s study being the first to investigate RAB7's autophagic role in skeletal muscle physiology, the conclusions drawn from these experiments cannot be directly

translated to mammalian physiology, as some RABs have altered functions in different organisms. For example, while RAB7 takes part in ALF in Drosophila, it is unclear this is true in mammalian cells (37). The most recent study by Melendez, et al. (2021) found that electroporation-mediated expression of RAB7-T22N (dominant negative) in chicken embryos results in decreased dermomyotome-derived myoblast fusion (86). The researchers connected myoblast fusion deficits to inhibition of RAB7-dependent degradation of TGFβs (transforming growth factor, beta) which inhibit myoblast fusion (86). Although this study was the first to show that RAB7 regulates myoblast fusion, it was not determined if impairment of TGFβ degradation was directly connected to RAB7-mediated autophagy deficits. Furthermore, Melendez, et al. (2021) did not investigate the impact of RAB7 inhibition on (mammalian) myoblast differentiation (86).

While these studies set a strong foundation for RAB7 muscle physiology research, it is still unknown if RAB7 is critical for mammalian skeletal muscle physiology. Specifically, it is unknown if RAB7 is required for myoblast differentiation and fusion by mediating autophagy and mitophagy.

Chapter 2: Purpose and Study Design

2.1 Rationale and Purpose

Previous research has shown that both autophagy and mitophagy are indispensable for myoblast differentiation (10,12,13,29,31,32). Knockdown and knockout models of *Rab7* and other components of the RAB7 cycle (such as *Rab5*, *Ccz1*, and various RAB7 GAPs such as *Tbc1d2, 5, 15,* and *17*) lead to dramatic and consistent deficits in autophagy, PRKN-dependent, and PRKN-independent mitophagy (37,43,54,57-61,77-83). Furthermore, three studies exist that implicate RAB7 in skeletal muscle physiology; however, none explicitly connect RAB7-mediated autophagy and mitophagy to mammalian myoblast differentiation and fusion (84-86). Altogether, the evidence provided by all of these studies leads to my hypothesis that RAB7 is essential for C2C12 differentiation through facilitating multiple stages of autophagy and mitophagy.

2.2 Objectives

1. Characterize the content and localization of RAB5, CCZ1, RAB7, and RABGDI during C2C12 differentiation.
2. Determine the effect of RAB7 inhibition on myoblast differentiation and myogenesis.
3. Determine the effect of RAB7 inhibition on autophagy and autophagic flux.

2.3 Experimental Design

2.3.1 Experiment 1: Characterizing RAB7 Content and Localization

An *in-vitro* C2C12 myoblast model was used to determine the content and localization of 4 constituents of the RAB7 cycle, including RAB5, CCZ1, RAB7, and RABGDI through immunoblotting. Whole cell, cytosolic-enriched, and mitochondrial-enriched C2C12 samples were collected during proliferation and multiple time points over five days of differentiation.

2.3.2 Experiment 2: The Effect of RAB7 Inhibition on Myoblast Differentiation

Some samples were chronically treated with RAB7 nucleotide-binding competitive inhibitor called CID1067700 (CID). In other samples, RAB7 was transiently knocked down (siRAB7) through siRNA transfection. The impact of CID and siRAB7 on C2C12 differentiation was quantified through immunoblotting MYOG and MYH. Additionally, morphological differences (myoblast fusion and differentiation indices) between treated and control cells were quantified through fluorescent microscopy.

2.3.3 Experiment 3: The Effect of RAB7 Inhibition on Autophagy and Autophagic Flux

Various autophagy proteins such as LC3, SQSTM1, and ATG7 were analyzed through immunoblotting cells treated with CID, RAB7 siRNA, vehicle control (CTRL), or scramble control (Scr). For autophagic flux experiments, cells were treated with CQ 24-hours before collection. Proteasome fluorometric assays were completed to identify if there was any UPS compensation for faulty autophagy.

2.4 Hypotheses

It was hypothesized that:

1) Since autophagy and mitophagy increase once C2C12 differentiation is induced (10-13,29,31,32), and the RAB7 cycle is crucial for both processes (37,43,54,57-61,77-83), then RAB5, CCZ1, RAB7, and RABGDI content would increase as autophagic/mitophagic demands increased. Moreover, RAB5, CCZ1, and RAB7 would be primarily found in mitochondrial-enriched fraction, while RABGDI would be mostly found in the cytosolic fraction. After differentiation induction, RAB5 and RAB7 would be hypothesized to localize to an even greater extent to the mitochondrial-enriched fraction as both autophagy and mitophagy increase.
2) Chemical inhibition and genetic knockdown of *Rab7* would lead to substantial deficits in differentiation and myogenesis. This would be shown by observing decreases in MYOG and MYH content, decreased fusion and differentiation indices, and fewer cells with greater than 3 nuclei.
3) Treatment with CID or siRAB7 would result in autophagic dysregulation such as decreased autophagic flux and autophagosome/autolysosome accumulation, resulting in UPS compensation. This would be shown by observing decreased LC3-II and SQSTM1 content in CQ experiments, increased LC3-II content towards late differentiation, and increased UPS activity in the treated groups (CID and siRAB7) compared to the controls (CTRL and Scr).

Chapter 3: Methods

3.1 Cell Culture

Mouse C2C12 skeletal myoblasts (ATCC, CRL-1772) were grown on polystyrene dishes (SarstedT) and cultured at 37ºC in growth media (GM) made from low-glucose Dulbecco's Modified Eagle's Medium (DMEM; D6046-500ML, Sigma Aldrich), 5% fetal bovine serum (FBS; F1051-500ML, Sigma Aldrich), 5% serum plus-II (14009C-500ML, Sigma Aldrich) and 1% penicillin/streptomycin (P/S;P0781-100ML, Sigma Aldrich) with 5% CO_2. Once the cultures were ~80% confluent, differentiation was induced by substituting GM with differentiation media (DM), which was replaced daily. DM is made from DMEM, 2% horse serum (H0146, Sigma Aldrich) and 1% penicillin/streptomycin. Cells were collected prior to and every 24 hours after DM substitution – 0h (D0), 24h (D1), 48h (D2), 72h (D3), 96h (D4), and 120h (D5).

3.2 Chronic Drug Treatment

Some cells were incubated with 2.5µM of RAB7 nucleotide-binding chemical inhibitor (CID1067700; Axon Medchem, 2184) or dimethyl sulfoxide (DMSO) vehicle control (CTRL) starting at 24 hours (or 48 hours for CQ experiments) before D0 collection (~40% confluency). To assess autophagic flux, cells were treated with 40µM of CQ 24 hours before collection. Proteins analyzed during flux experiments (LC3-II and SQSTM1) are displayed as "net flux". This measure represents the net CQ-induced changes in autophagic proteins. This is calculated by taking the difference between samples with and without CQ within the same experimental group and normalizing them to D0 CTRL (or Scr) + CQ.

3.3 Transient Expression of RAB7 siRNA

Some cells were transfected 24 hours (or 48 hours for CQ experiments) before D0 with siRNA (siRAB7) against RAB7 or a scramble (Scr) control (Santa Cruz Biotechnology; sc-270071 and sc-37007, respectively) using JetPrime transfection reagents (Polyplus Transfection; 114-07) according to the manufacturer's instructions. Briefly, the siRNA, JetPrime buffer, JetPrime transfection reagent were mixed and incubated for 10 minutes at 22°C. Cells were left to incubate in GM containing 100μL of the transfection mixture with siRNA at 37°C for 24 hours, that was then replaced with fresh GM. Immunoblotting of RAB7 was used to determine siRNA transfection efficiency.

3.4 Preparation of Cell Lysates and Enriched Subcellular Fractions

For whole cell lysates, cells were trypsinized (0.25% trypsin with 0.2 g/L EDTA; Sigma Aldrich, T4049-500ML), centrifuged for 5 minutes at 1000g, and stored at -80°C. Lysis buffer [10mM NaCl, 1mM DTT, 1.5mM MgCl, 20mM HEPES, 0.1% Triton-X100 (BioShop, TRX506), 20% Glycerol (pH 7.4)] and protease inhibitor cocktail (Roche Applied Sciences, 04693116001) were added to the immunoblotting samples that were sonicated for 12 seconds. For assay samples, the same process was done in absence of protease inhibitor cocktail.

Mitochondrial and cytosolic enriched subcellular fractions were collected by suspending trypsinized cells in digitonin buffer (250mM sucrose, 80mM KCl, and 50 μg/mL digitonin; Sigma Aldrich D141 in PBS) for 5 minutes at 4°C. Cells were centrifugated for 10 minutes at 1000g, the supernatant was further centrifugated for 10 minutes at 16000g. The supernatant was the cytosolic-enriched fraction. The pellet from the 1000g spin was washed with lysis buffer,

centrifugated for 10 minutes at 1000g, incubated for five minutes at 4°C, then the supernatant was spun again at 1000g for 10 minutes. The resulting supernatant was the mitochondrial-enriched fraction. Both enriched fractions received 5μL of protease inhibitor cocktail. Immunoblotting CuZnSOD/SOD1 (superoxide dismutase 1, soluble; cytosolic) and MnSOD/SOD2 (superoxide dismutase 2, mitochondrial) (Enzo Life Sciences, SPA-810 and BML-SA115 respectively) were used to determine subcellular fraction purity.

3.5 Immunoblot Analysis

Cell lysate samples containing equal amounts of total protein, as determined through BCA protein analysis, were loaded and separated using 7.5-15% SDS-PAGE gels prior to a 30-minute transfer onto PVDF membranes (Bio-Rad Laboratories). PVDF membranes underwent a one-hour block in 5% milk-TBST (Tris buffer saline tween 20) [(20 mM Tris, 137 mM NaCl, pH 7.5)-0.1% Tween 20 (BioShop, TWN508)] solution followed by an overnight incubation in a 5% milk-TBST solution at 4°C containing appropriate primary antibodies. The antibodies used included RAB7(A), RAB5, CCZ1, BNIP3, RABGDI, (Santa Cruz Biotechnology; sc-376362, sc-46692, sc-514290, sc-56167, and sc-374649, respectively), MYH, MYOG (Developmental Studies Hydridoma Bank; MF20, and F5D, respectively), GAPDH (glyceraldehyde-3-phosphate dehydrogenase), LC3B, ATG7 (Cell Signaling Technologies; cs-2118, cs-2775, and D12B11 respectively), and SQSTM1 (MBL International; PM045). After washing with TBST, the membranes are incubated with the corresponding horseradish peroxidase (HRP)-conjugated secondary antibody (Biorad 1706515 and 1706516) for one hour at room temperature. After further TBST washes, the membranes were then coated in Clarity ECL blotting substrate

(BioVision, K820-500) for three minutes at room temperature. The bands were detected through UV exposure and pictures were taken using the ChemiDoc MP Imaging System (Biorad Laboratories). The molecular weights were estimated by Precision Plus Protein WesternC Standards (Biorad Laboratories, 161–0376).

3.6 Proteasome Fluorometric Assay

To identify the chymotrypsin-like activity of the proteasome, C2C12 whole cell lysates without protease inhibitor were incubated in assay buffer (1 mM $MgCl_2$, 10 mM NaCl, 25 mM KCl, 50 mM Tris/HCl, pH 7.5) with fluorogenic substrate Suc-LLVY-AMC (Enzo Life Sciences, BML-P802) for 1 hour at 30°C in darkness. All samples were loaded into black 96-well plates, where half of the samples had proteasome inhibitor called epoxomicin (Cayman Chemical, 10007806). Fluorescence was measured using the Cytation 5 imager (BioTek) with an excitation wavelength of 360nm and an emission wavelength of 460nm. Proteasome activity was quantified by taking the difference between samples incubated with and without the proteasome inhibitor, where the values are then normalized to protein content as determined through BCA.

3.7 Myoblast Fusion and Differentiation Indices

To identify differences in myoblast differentiation and myogenesis, while still adhered to the 12-well polystyrene plate, cells were washed with PBS and fixed with 300μL of 4% formaldehyde for 10 minutes. After aspirating the supernatant, the cells were permeabilized with 0.1% Triton X-100 for 10 minutes at 22°C. After aspirating again, 10% goat serum (GS; Sigma-Aldrich, G9023)-PBS blocking solution was added to the cells for 30 minutes. The GS blocking solution was replaced with 1:200 MYH primary antibody (MF20; Developmental Studies Hybridoma

Bank) in 10% GS and left to incubate for 2 hours at 22°C on a shaker (120rpm). After aspirating the MYH-GS solution and three 3-minute PBS washes, 1:500 anti-mouse PE-conjugate secondary antibody (sc-3738, Santa Cruz Biotechnology) in 10% GS was added and left to incubate for 1 hour. After another three 3-minute PBS washes, cells were stained with 1:50 DAPI (D1306, Invitrogen) for 5 minutes at 22°C. Three more 3-minute washes with PBS were done before imaging on the Cytation 5 imager (BioTek). The differentiation index was determined by calculating the ratio of the number of fluorescent MYH-positive cells to non-fluorescent MYH-negative cells. The fusion index was determined by calculating the ratio of the number of mono- to multi-nucleated cells. A similar approach to the fusion index was used for calculating the ratio of cells with greater than or equal to 3 nuclei.

3.8 Statistics

One-way ANOVA tests were used to assess the effects of differentiation within groups. A Bonferroni post hoc was used to determine statistically significance differences between D0 and the other time points. To compare differences between time-matched conditions, a series of unpaired two-tailed Student t-tests were used. For all experiments $*p < 0.05$ was considered significantly different within the group and a $^{\dagger}p < 0.05$ between groups, while $p<0.10$ was considered a non-significant trend. The results are presented as the mean ± SEM.

Chapter 4: Results

4.1 Differentiation Induces Changes to the RAB7 Cycle

To elucidate the impact of C2C12 differentiation on the RAB7 cycle, four constituents of this pathway (RAB5, RAB7, CCZ1, and RABGDI) were analyzed through immunoblotting. When C2C12 cells differentiate, as indicated by increasing MYH content, RAB7, RAB5, and RABGDI content rose during mid- to late- differentiation (**Figure 4A-B**). CCZ1 was constant throughout C2C12 differentiation (**Figure 4A-B**). To elaborate, there were significant ($p<0.05$) 15- to 18-fold increases of RAB5 at D4 and D5, 2.6- to 3.2-fold increases of RAB7 at D2 and D3, and 2.2- to 3.5-fold increases of RABGDI at D2-D5 (**Figure 4A-B**). While RAB5 and MYH content gradually increased throughout myoblast differentiation, RAB7 and RABGDI content peaked at D3, where the former was no longer significantly ($p>0.05$) different from D0 at D4 and D5 (**Figure 4A-B**).

Some proteins of the RAB7 cycle changed where they localized during differentiation. RAB5 and RABGDI localized to the cytosolic fraction (CF) to a significantly ($p<0.05$) greater extent than the mitochondrial fraction (MF) during early differentiation (**Figure 4C-E**). However, during mid- to late-myoblast differentiation, these differences quickly dissipated, whereby D5 RABGDI has nearly equal content in both fractions and RAB5 has significantly ($p<0.05$) more content in the MF (**Figure 4C-E**). RAB7 localizes to the MF significantly ($p<0.05$) more than the CF during the entire 5-day time-course (D0-D5), whereas CCZ1 tends ($p<0.1$) to increase CF content after differentiation is induced (D1-D4) (**Figure 4C-E**). Differentiation leads to increases in RAB5 MF ($p<0.05$), RAB7 MF ($p<0.05$), RABGDI MF ($p<0.05$), and CCZ1 CF ($p<0.1$) content, as well as decreases in RAB7 CF ($p<0.05$) and RABGDI CF ($p<0.05$) content, whereas CCZ1 MF ($p>0.05$) and RAB5 CF $p>0.05$) remained

unchanged (**Figure 4C-E**). MnSOD and CuZnSOD were used as CF and MF purity controls, respectively (**Figure 4D**).

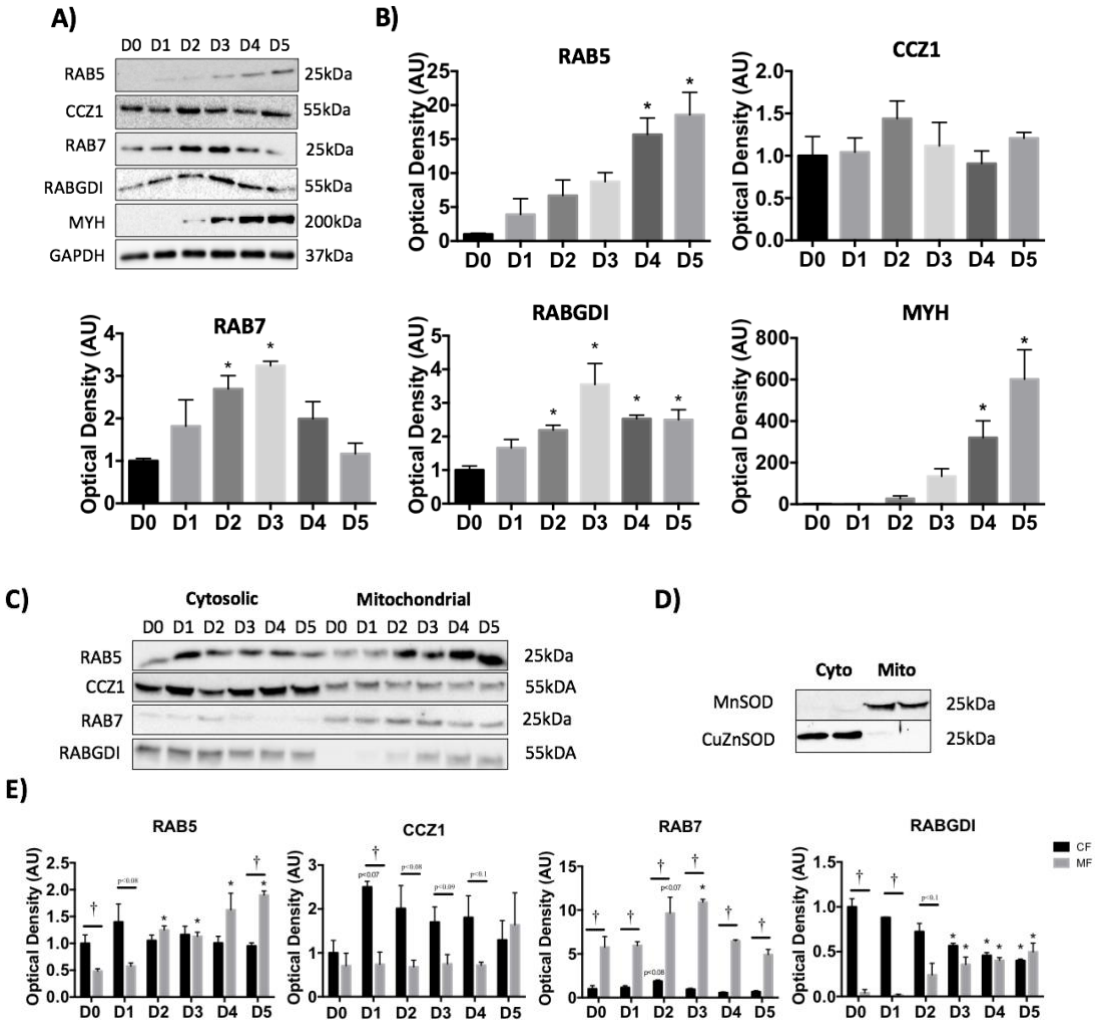

Figure 4: RAB5, RAB7, and RABGDI Content Changes Over Differentiation.

(**A,C**) Representative immunoblots and (**B,E**) quantification of RAB5, CCZ1, RAB7, and RABGDI protein content in whole cell (**A**,**B**) and fractions (**C-E**) over D0-D5 of C2C12 myoblast differentiation. **B** was normalized to D0, while **E** was normalized to cytosolic D0. GAPDH was the loading control (**A**), MYH was used as a differentiation control (**A**), and MnSOD and CuZnSOD (**D**) were used as fraction purity controls. Significant differences between D0 and other timepoints were calculated through one-way ANOVA, while significant differences between groups was calculated by two-tailed T-tests. The former was denoted by *$p<0.05$ and the latter by $^{\dagger}p<0.05$. [n=2-4 independent experiments, mean ± SEM]

4.2 Chronic CID Treatment Negligibly Alters the RAB7 Cycle

Chronically treating cells with 2.5μM of CID starting 24 hours before D0 results in negligible, insignificant ($p>0.05$) changes to RAB5, RAB7, and RABGDI content throughout most of differentiation (**Figure 5A-B**). Both RAB5 and RABGDI tended ($p<0.1$) to increase by about 50% in the CID treated group at D0 compared to CTRL (**Figure 5A-B**). RAB5 was also significantly ($p<0.05$) decreased at D5 in the CID group by about 20% (**Figure 5A-B**).

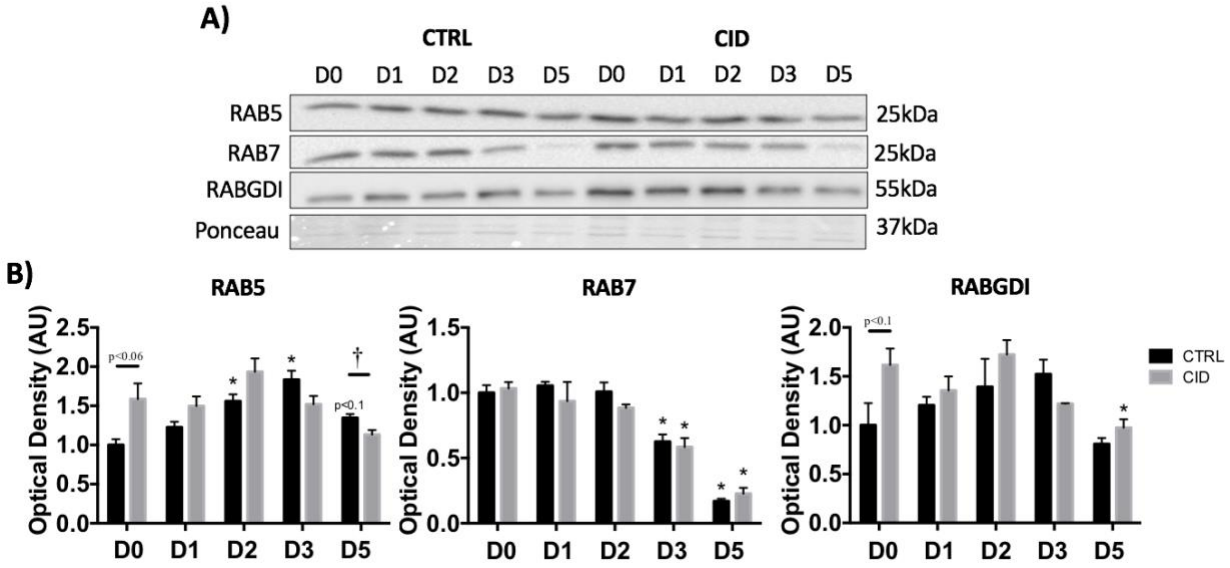

Figure 5: The RAB7 Cycle Remains Relatively Stable After CID Treatment

C2C12 myoblasts were chronically treated with either vehicle control (CTRL) or CID starting at -D1. (**A**) Representative immunoblots and (**B**) quantification of RAB5, RAB7, and RABGDI protein content normalized to D0 of the CTRL group over D0-D5 of C2C12 myoblast differentiation in whole cell lysates. Ponceau was the loading control. Significant differences between D0 and other timepoints were calculated through one-way ANOVA, while significant differences between groups was calculated by two-tailed T-tests. The former is denoted by *$p<0.05$ and the latter by $^{\dagger}p<0.05$. [n=4 independent experiments, mean ± SEM]

4.3 Chronic CID Treatment Results in Reduced Myoblast Differentiation and Myogenesis

Western blot analysis revealed that both groups experienced a significant ($p<0.05$) 4.2- to 7.4-fold increase in MYOG content during mid differentiation (specifically at D1-D3) when compared to D0 (**Figure 6A-B**). There were no significant ($p>0.05$) differences in MYOG

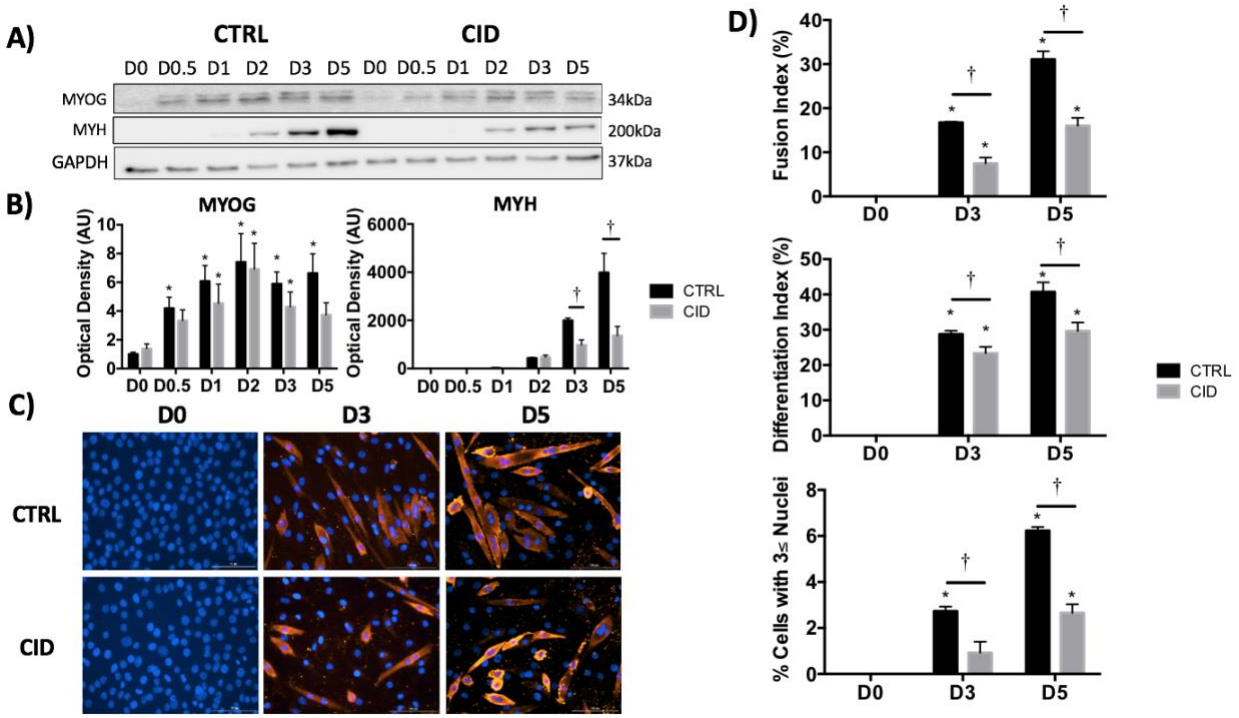

Figure 6: Myoblast Differentiation and Myogenesis After Chronic CID Treatment

C2C12 myoblasts were chronically treated with either vehicle control (CTRL) or CID starting at -D1. (**A**) Representative immunoblots and (**B**) quantification of MYOG and MYH content normalized to D0 of the CTRL group in whole cell lysates, where GAPDH is the loading control. (**C**) Representative fluorescent microscopy images where nuclei are stained in blue (DAPI) and MYH is stained red (PE). (**D**) Quantification of fusion and differentiation indices, and the number of cells with ≤3 nuclei using Gen5 (3.08) software. Significant differences between D0 and other timepoints were calculated through one-way ANOVA, while significant differences between groups was calculated by two-tailed Student t-tests. The former is denoted by *$p<0.05$ and the latter by $^{\dagger}p<0.05$. [n=3-4 independent experiments, mean ± SEM]

between CTRL and CID-treated cells (**Figure 6A-B**). MYH was significantly ($p<0.05$) increased at D3 and D5 for both groups, however, when compared to the control, the CID group had 51-66% less MYH content at D3 and D5 than the CTRL group ($p<0.05$; **Figure 6A-B**). Immunofluorescent microscopy showed that the fusion and differentiation indices became significantly ($p<0.05$) elevated in both groups after 3 and 5 days of differentiation (**Figure 6C-D**). However, CID-treated cells show significant reductions in multiple morphological measures when compared to the CTRL (**Figure 6C-D**). Specifically, there was a 19-27% decrease in the differentiation index, a 48-55% decrease in the fusion index, and a 57-66% decrease in the number of cells that have greater than 2 nuclei at D3 and D5 ($p<0.05$; **Figure 6C-D**).

4.4 Autophagy is Disrupted After Chronic CID Treatment

Although LC3-I and LC3-II/LC3-I ratio was largely unaltered, LC3-II content was significantly ($p<0.05$) increased after inducing differentiation (**Figure 7A-B**). Immunoblotting showed that LC3-II was elevated in the CTRL group at D0.5-D3 of differentiation, and in the CID group at D2 and D3 (**Figure 7A-B**). Additionally, CID treated cells had 47-75% more LC3-II compared to the CTRL at D0 and D2-D5 ($p<0.05$; **Figure 7A-B**). SQSTM1 experienced a drastic and significant ($p<0.05$) decrease in both groups once differentiation was induced (**Figure 7A-B**). CID-treated cells had 52-63% less SQSTM1 content at D0 ($p<0.05$) and D1 ($p<0.1$) than the CTRL group, however these differences diminish at all other timepoints (**Figure 7A-B**). To determine if there are alterations to the UPS system caused by alterations in autophagy, proteasome activity was analyzed. At D0, proteasome activity was significantly ($p<0.05$) decreased by 45% in the CID group compared to CTRL, however this observation faded by D1

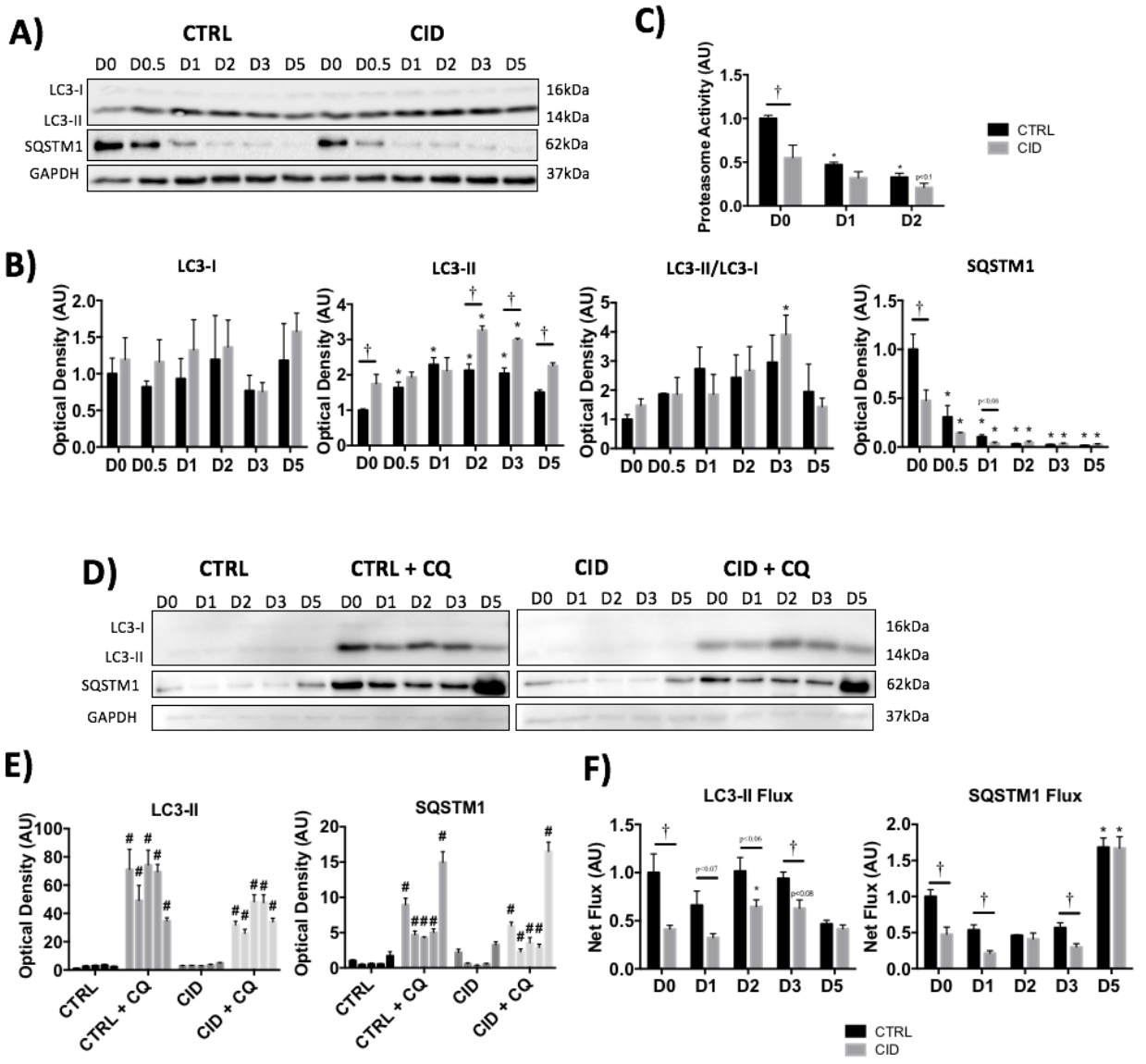

Figure 7: CID-Mediated Autophagic Deficits

C2C12 myoblasts were chronically treated with either vehicle control (CTRL) or CID starting at -D1 for **A-C** and -D2 for **D-F**. (**A,D**) Representative immunoblots and (**B,E**) quantification of LC3 and SQSTM1 content in (**A,B**) whole cell lysates without and (**D,E**) with CQ treatment, where GAPDH is the loading control. (**C**) Quantification of proteasome activity through a fluorometric assay after normalizing to total protein content. (**F**) Quantification of the CQ-induced net flux of LC3-II and SQSTM1. **B, C, E** and **F** were normalized to D0 of the CTRL group. *$p<0.05$ compared to D0 (within group), $^{\dagger}p<0.05$ between groups at the same time point, $^{\#}p<0.05$ comparing the same experimental group at the same time point between CQ and non-CQ experiments. [n=3-4 independent experiments, mean ± SEM]

(**Figure 7C**). Next, CQ experiments were conducted to identify if CID treatment would lead to alterations in autophagic flux. As seen in **Figure 7D-E**, 24-hour incubation with 40µM of CQ led to stark significant ($p<0.05$) increases LC3-II and SQSTM1 content in the CTRL CQ and CID CQ groups compared to their time-matched non-CQ treated counterparts. When analyzing the net (CQ-induced) flux, CID treated cells had consistent decreases in LC3-II by 33-59% between D0-D3 when compared to the control (D0 and D3; $p<0.05$, D1 and D2; $p<0.1$; **Figure 7F**). Furthermore, the CID group experienced significant ($p<0.05$) decreases in SQSTM1 content by 47-60% at D0, D1, and D3 compared to the CTRL group (**Figure 7F**).

4.5 siRAB7 Results in Minimal Changes to the RAB7 Cycle

Western blot analysis showed that RAB7 siRNA transfection resulted in a significant ($p<0.05$) decrease in RAB7 content by 67-95% compared to the Scr (**Figure 8A-B**). *Rab7* knockdown resulted in no changes in RAB5 or CCZ1 content between groups during differentiation ($p>0.05$; **Figure 8A-B**). However, siRAB7 results in elevated RABGDI content at D2 ($p<0.1$) and D3 ($p<0.05$; **Figure 8A-B**).

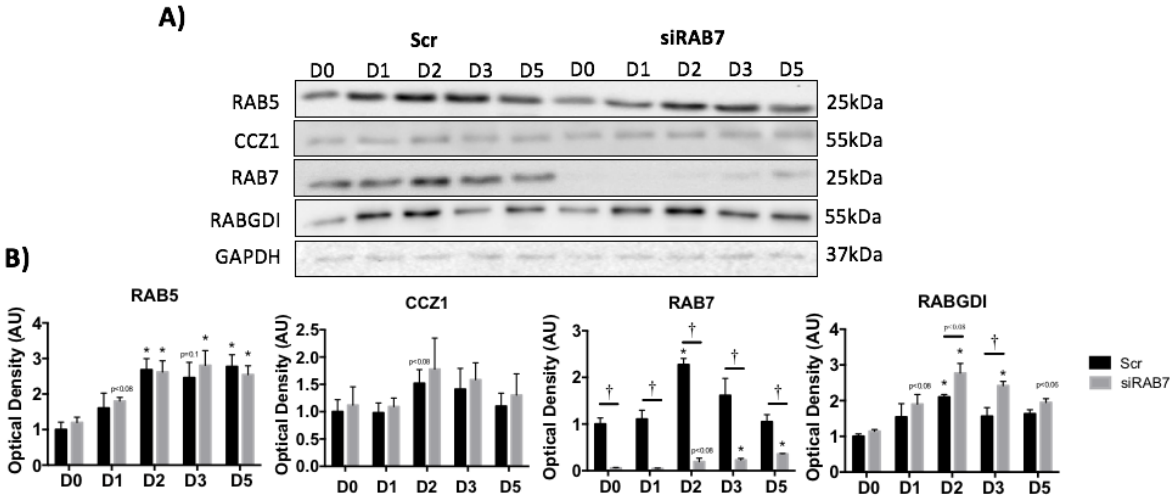

Figure 8: The RAB7 Cycle After siRAB7 Transfection

C2C12 myoblasts were treated with either scramble control (Scr) or siRAB7 starting at -D1. (**A**) Representative immunoblots and (**B**) quantification of RAB7, RAB5, and RABGDI protein content normalized to D0 of the Scr group in whole cell lysates over the course of 5 days of differentiation. GAPDH was used as a loading control. *p<0.05 compared to D0 (within group). [n=3 independent experiments, mean ± SEM]

4.6 siRAB7 Dramatically Reduces Myoblast Differentiation and Myogenesis

Immunoblotting showed that although MYOG is significantly ($p<0.05$) elevated during mid-differentiation (D2-D3) in the Scr and siRAB7 groups, there are no significant differences between groups ($p>0.05$; **Figure 9A-B**). MYH increased at D3 in Scr cells ($p<0.1$) and at D5 ($p<0.05$) in both experimental groups, although, the siRAB7 group had 48-53% less MYH content at D2 ($p<0.05$), D3 ($p<0.1$) and D5 ($p<0.05$) than the Scr (**Figure 9A-B**). Furthermore, immunofluorescent microscopy showed that siRAB7 results in significant ($p<0.05$) decreases in morphological characteristics. Specifically, there was a 48-49% decrease in the differentiation index, an 80-90% decrease in the fusion index, and a 91-94% decrease in the number of cells that have greater than 2 nuclei at D3 and D5 ($p<0.05$; **Figure 9C-D**).

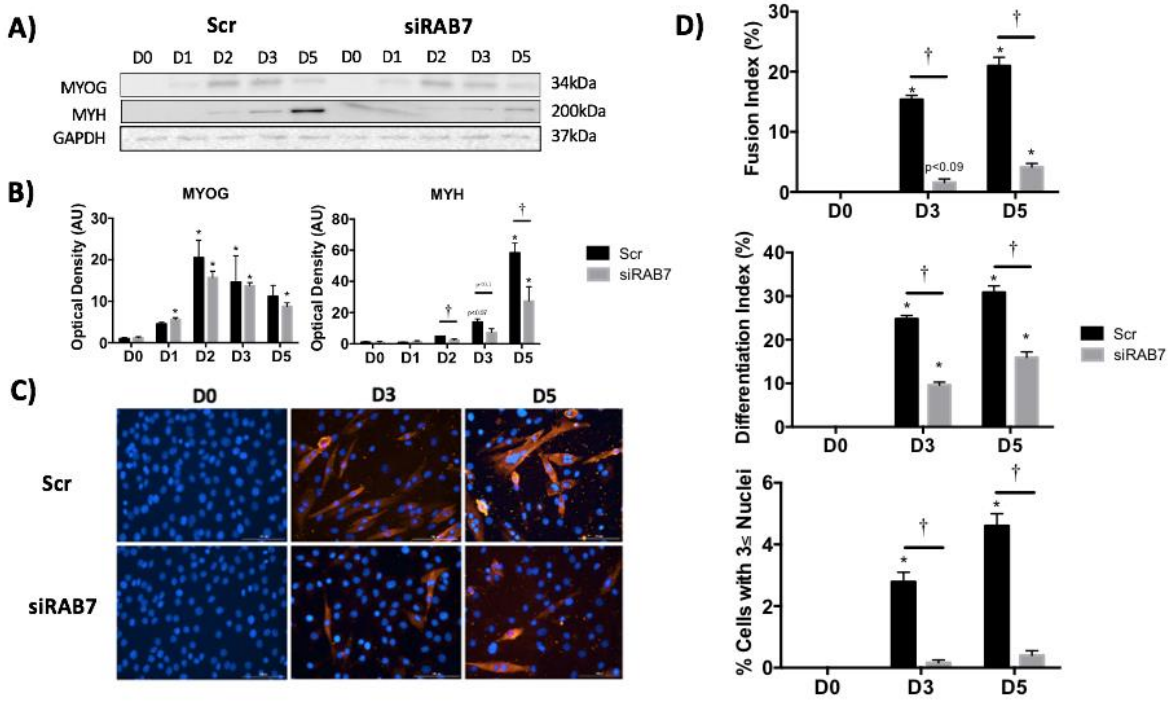

Figure 9: Myoblast Differentiation and Myogenesis After siRAB7 Transfection

C2C12 myoblasts were treated with either scramble control (Scr) or siRAB7 starting at -D1. (**A**) Representative immunoblots and (**B**) quantification of MYOG and MYH content normalized to D0 of the Scr group in whole cell lysates, where ponceau is the loading control. (**C**) Representative fluorescent microscopy images where nuclei are stained in blue (DAPI) and MYH is stained red (PE). (**D**) Quantification of fusion and differentiation indices, and the number of cells with ≤3 nuclei using Gen5 (3.08) software. Significant differences between D0 and other timepoints were calculated through one-way ANOVA, while significant differences between groups was calculated by two-tailed Student t-tests. The former is denoted by *$p<0.05$ and the latter by $^{\dagger}p<0.05$. [n=3-4 independent experiments, mean ± SEM]

4.7 Autophagy is Disrupted After *Rab7* Knockdown

Western blot analysis showed that there was a significant ($p<0.05$) 37% decrease in ATG7 and a significant ($p<0.05$) 44% decrease in LC3-I in siRAB7 cells compared to Scr at D2 of differentiation (**Figure 10A-B**). Despite both groups having significantly ($p<0.05$) less SQSTM1 after the induction of differentiation, there were significant ($p<0.05$) differences in SQSTM1

content between groups at D0, D3, and D5 (**Figure 10A-B**). Specifically, there was 37% less SQSTM1 in the siRAB7 group at D0, and 188-250% more in the siRAB7 group at D3 and D5 (**Figure 10A-B**). Both Scr and siRAB7 cells had significantly ($p<0.05$) more LC3-II content during mid- to late-differentiation (specifically D2-D5; **Figure 10A-B**). However, siRAB7 cells had more LC3-II at D2 (61%, $p<0.1$), D3 (112%, $p<0.05$), and D5 (119%, $p<0.05$; **Figure 10A-B**). Furthermore, these differences persisted when measuring the LC3-II/LC3-I ratio. D2-D5 of the siRAB7 group and D3 of the Scr group experience significant ($p<0.05$) increases in LC3-II/LC3-I ratio compared to D0 (**Figure 10A-B**). The LC3-II/LC3-I ratio was significantly ($p<0.05$) elevated in siRAB7 cells compared to Scr cells from D1-D5 by 55-202%, where the largest differences tended towards late differentiation (**Figure 10A-B**). Next, proteasome activity was analyzed to identify if there is a shift in the autophagy-UPS balance. Although insignificant, there was consistently less (by 44-47%) proteasome activity in siRAB7 cells compared to the Scr. Specifically, there was 44% less at D0 ($p<0.1$), 47% less at D1, and 44% less at D2 ($p>0.1$) (**Figure 10C**). Finally, to determine if autophagic flux is altered in the absence of RAB7 (verified in **Appendix A**), CQ experiments were conducted. As seen in **Figure 10D-E**, both Scr and siRAB7 groups experienced a significant ($p<0.05$) increase in LC3-II and SQSTM1 content across most of differentiation when compared to their time matched non-CQ treated counterparts. However, this observation excludes the increase in SQSTM1 at D1 in the Scr ($p<0.1$), and the decreases in both LC3-II ($p<0.1$) and SQSTM1 ($p>0.1$) content at D5 in the siRAB7 cells (**Figure 10D-E**). When analyzing the net (CQ-induced) flux, there were no significant ($p>0.05$) differences between groups for most of differentiation (**Figure 10F**). However, there tended ($p<0.1$) to be 16% less LC3-II flux at D0, and at D5 there was

significantly ($p<0.05$) less LC3-II and SQSTM1 flux by 74% and 20% respectively at D5 (**Figure 10F**).

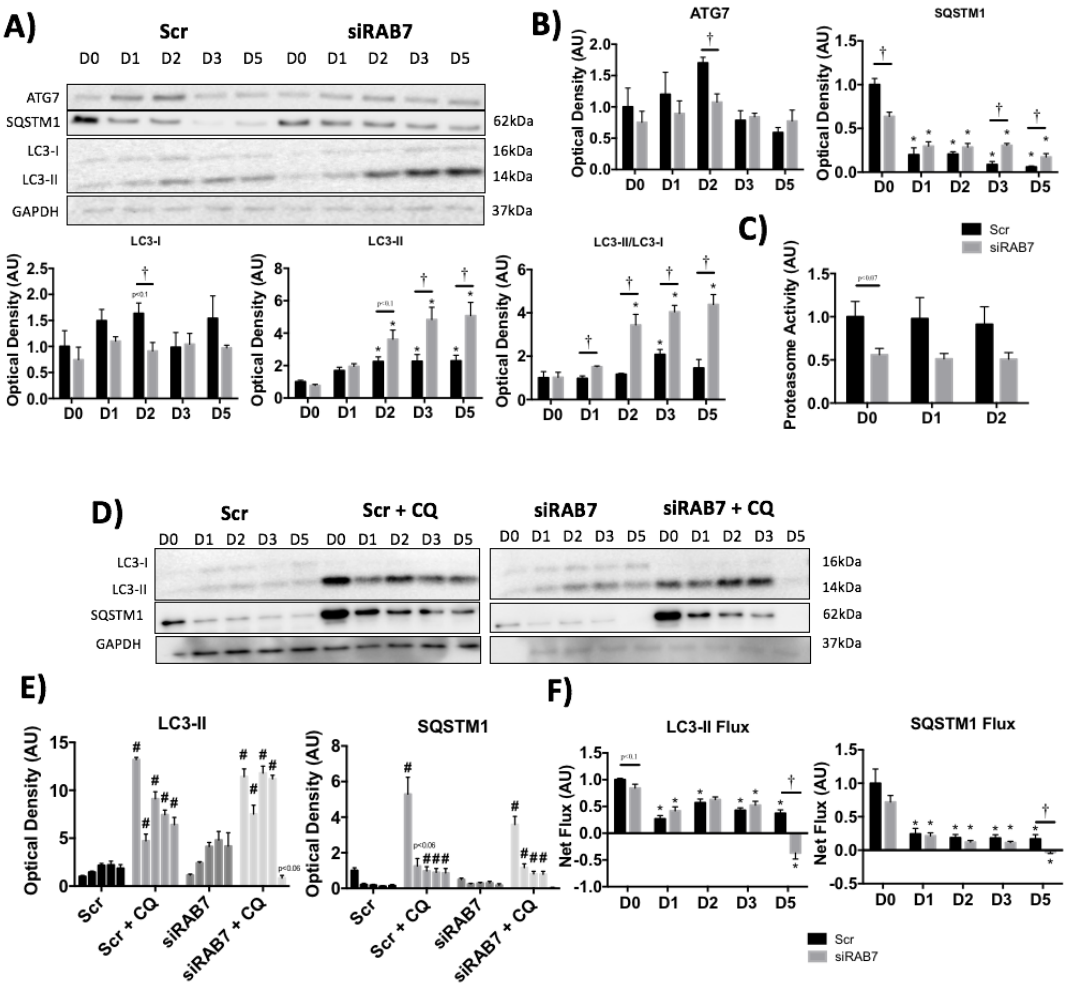

Figure 10: RAB7 siRNA-Mediated Autophagic Deficits

C2C12 myoblasts were treated with either scramble control (Scr) or siRAB7 starting at -D1 for **A-C** and -D2 for **D-F**. (**A,D**) Representative immunoblots and (**B,E**) quantification of LC3 and SQSTM1 content in (**A,B**) whole cell lysates without and (**D,E**) with CQ treatment, where GAPDH is the loading control. (**C**) Quantification of proteasome activity through a fluorometric assay after normalizing to total protein content. (**F**) Quantification of the CQ-induced net flux of LC3-II and SQSTM1. **B, C, E,** and **F** were normalized to D0 of the Scr group. *$p<0.05$ compared to D0 (within group), $^{\dagger}p<0.05$ between groups at the same time point, $^{\#}p<0.05$ comparing the same experimental group at the same time point between CQ and non-CQ experiments. [n=3-4 independent experiments, mean ± SEM]

Chapter 5: Discussion

5.1 Study Scope

The primary focus of this study was to examine the importance of RAB7 in C2C12 differentiation and myogenesis by mediating autophagy. Despite how RAB7 participates in multiple mechanisms that are critical for skeletal muscle physiology, only three studies exist that connects RAB7 to this phenomenon (84-86). While these studies create a firm foundation, none provide evidence on whether RAB7 is critical for mammalian myoblast differentiation and fusion. Furthermore, only one of these studies demonstrates that morphological differences due to RAB7 (genetic) interference was caused by autophagic deficits (85), while another implied this but provided no evidence (86). Thus, this study was designed to elucidate the impact of RAB7 on mammalian myoblast differentiation by facilitating autophagy.

5.2 C2C12 Differentiation Induces Changes to RAB7 Cycle Protein Content and Localization

In order to test the hypothesis that RAB7 is critical for C2C12 differentiation and myogenesis, the RAB7 cycle first needed to be characterized during this process. Four constituents of the RAB7 cycle were analyzed, including RAB5, CCZ1, RAB7, and RABGDI through western blot. These specific proteins were analyzed because they are four of the six proteins that are consistent in most RAB7-dependent mechanisms. The other two proteins, RABGEF1 and MON1, were not observed because measuring both MON1 and CCZ1 is redundant; they are both required to form the MON1-CCZ1 complex which then participates in the RAB7 cycle (43). As for RABGEF1, its major function in the RAB7 cycle is to adhere RAB5 to membranes (43). Characterizing RABGEF1 content will not provide much novel information for two reasons. First, changes in

RABGEF1 do not directly translate to changes in RAB5 activation or localization. Second, RAB5 localization and content were already being tested, so having RABGEF1 data is largely redundant. Additionally, the TBC1D family of proteins were not analyzed because many of them act as RAB7-GAPs depending on the function-specific circumstance. For example, TBC1D2, TBC1D5, and TBC1D15 all act as RAB7-GAPs in different circumstances (summarized by 34).

Progressive increase of MYH content served as an indicator of C2C12 differentiation (7,8,10-13). Once differentiation was induced, RAB5 content progressively increased over the five-day time course. Despite being downstream of RAB5, both RAB7 and CCZ1 followed different trends. RAB7 protein content increased until D2-D3 and then declined to pre-differentiation (D0) levels by D5, whereas CCZ1 content remained unchanged throughout. RABGDI followed a similar trend to RAB7; however, at D4 and D5 the content remained elevated compared to D0. These results were unexpected for multiple reasons, the first being the discrepancy in the protein content patterns between RAB5 and RAB7. Current studies suggest that RAB5 mechanisms lead to downstream RAB7-dependent processes such as autophagy, mitophagy, and endocytosis (43,47,77). Since RAB7 replaces RAB5 in most of these mechanisms, then it is reasonable to predict that they have similar protein expression patterns, but this was not the case in differentiating C2C12 cells. The differences in RAB5 and RAB7 content patterns during differentiation suggest that there may be RAB5-dependent processes that exist independently of RAB7, and/or the efficiency of RAB7 recycling increases during mid- to late-differentiation. Another unexpected result was that CCZ1 protein expression had no changes throughout differentiation despite both RAB5 and RAB7 content increasing at some point during this process. Since CCZ1 facilitates the replacement of RAB5 with RAB7, then CCZ1 content

should increase similarly to RAB5 or RAB7. However, CCZ1 content was unaltered during differentiation indicating that CCZ1 recycling is rapid and that there is an inactive pool prepared for activation. The pattern of RABGDI content was as predicted. Since RABGDI interacts with multiple RABs including RAB5 and RAB7, it is logical that the protein expression pattern was a hybrid of the two. In sum, C2C12 differentiation induces changes in RAB5, RAB7, and RABGDI content, suggesting an intimate connection between the RAB7 cycle and myoblast differentiation.

To gain further insight into the relationship between the RAB7 cycle and C2C12 differentiation, cytosolic and mitochondrial-enriched subcellular fractions were analyzed. Fractionation experiments revealed that differentiation induces dynamic changes in subcellular localization for most of the constituents of the RAB7 pathway. As previous papers have claimed, cytosolic RABs are inactive, while RABs attached to membranal organelles, such as the mitochondria, are active (43,47). Although this logic is not directly transferable to CCZ1 or RABGDI (43), determining subcellular localization of these proteins can still provide valuable information such as recycling rates and the existence of cytosolic pools.

Subcellular fractionation experiments demonstrated 4 important findings in relation to differentiation-induced changes in RAB7 cycle localization. To start, at D0 and during early differentiation, RAB5 and RABGDI are more localized to the cytosol. Both RAB5 and RABGDI had progressively increasing protein content in mitochondrial-enriched fractions. Differentiation resulted in unaltered RAB5 cytosolic content and decreasing RABGDI cytosolic content. RAB5 fractionation data suggests that RAB5 demand and activity level increased over the course of differentiation, while an inactive and unchanging cytosolic pool exists to ensure that RAB5 is

readily available. RABGDI localizes to the cytosol when attached to inactive RAB proteins to help solubilize and transport them (43). The localization shift in RABGDI from the cytosol to mitochondrial-enriched fractions suggests that the recycling of various RABs increased throughout differentiation, as there is less of a need for RABGDI to remain in the cytosol. A similar conclusion can be drawn from the localization of CCZ1. There is negligible change in the mitochondrial localization of CCZ1, however differentiation induced an increase in cytosolic CCZ1. Currently, no known cytosolic MON1-CCZ1 function exists. Thus, this increase in cytosolic content and maintenance of mitochondrial-enriched CCZ1 suggests that CCZ1 recycling becomes upregulated once differentiation is induced, as there is a larger cytosolic pool available. RAB7 localized to the mitochondrial-enriched fractions to a much greater extent than the cytosolic fraction. This finding indicates that RAB7 demand and activity level is high in C2C12 cells before and throughout differentiation. Similarly to that of RAB5, RAB7's cytosolic content was consistent throughout differentiation to ensure that the inactive RAB7 pool does not deplete and is free to participate in the RAB7 cycle. Together, this fractionation data provides four major pieces of information. The first is that, although future studies should verify these findings, differentiation-induced changes in RAB activity based on its localization can be estimated. The second is that RAB5, RAB7, CCZ1, and RABGDI cytosolic pools exist to ensure that inactive versions of these proteins are always available and readily recruitable. Third, changes in RAB5 and RAB7 content do not increase the size of the cytosolic pool, but rather are concentrated to the active mitochondrial-enriched fraction. And last, RAB5 and RAB7 localize to the mitochondria, indicating that the RAB7 cycle likely has a role in mitochondrial dynamics (especially mitophagy) in C2C12 cells.

Altogether, changes in localization and protein content seen in **Figure 4** demonstrate that the RAB7 cycle is inherently connected to C2C12 differentiation. To further elucidate the importance of the RAB7 cycle in myoblast differentiation, C2C12 cells were treated with RAB7 chemical inhibitor (CID) and knocked down through RAB7 siRNA transfection.

5.3 CID and siRAB7 Leads to Negligible Changes in the RAB7 Cycle

RAB5 and RABGDI content experienced little to no change throughout differentiation despite RAB7 being chemically inhibited or knocked down. RAB7 and CCZ1 also showed negligible change when comparing the experimental and control conditions. The main exceptions are found at D0 of RAB5 and RABGDI content in **Figure 5A-B**, and RABGDI at D2 and D3 in **Figure 8A-B**.

Any discrepancies seen between siRAB7 and CID were likely attributed to the specificity of the two inhibitory techniques. As tested by Agola, et al. (2012; 87), although CID inhibits RAB7, it is also not a specific drug. At 100nM RAB7 activity was lowered to 30% of baseline, but other GTP-binding proteins are also affected by 35-50% (87). As the author states "CID 10677000 is the first inhibitor with demonstrated activity against any member of the Rab subfamily of GTPases" (87). Thus, the increase in RAB5 and RABGDI seen at D0 in CID but not siRAB7 as well as the increase in RABGDI at D2-D3 in siRAB7 but not CID is likely due to the high specificity of RAB7 siRNA compared to the non-specific CID treatment.

Since CID prevents the nucleotide exchange of GDP to GTP on RAB7 (and to a lesser extent other RABs), elevations to RAB5 and RABGDI content at D0 were likely caused by a sudden cessation of RAB(7) activity. For example, if RAB5 was participating in the RAB7

cycle, but RAB7 could not be recruited properly by the MON1-CCZ1 complex due to its inability to become active (RAB7-GTP), then RAB5 would accumulate as seen at D0. As for RABGDI, upon a large influx of RAB-GDP, RABGDI content would increase to compensate, since RABGDI is required to solubilize and transport inactive RABs. These elevations in the CID group vanished by D1, suggesting that differentiation-induced adaptations caused RAB5 and RABGDI content to return back to normal. As suggested by Kuchitsu, et al. (2018; 57), other RABs could compensate for lack of active RAB7, although this has not been tested. However, if Kuchitsu, et al.'s hypothesis was true, it would explain the increase in RABGDI content in siRAB7 cells at D2 and D3. To elaborate, sufficient content of RABs other than RAB7, as well as their RABGDI-facilitated cytosolic emulsion and transport, may compensate for the lack of RAB7 activity. This elevation in RABGDI occurs at the same time as RAB7 reaches its peak content levels, thus providing evidence that there could be a RAB7-independent compensatory mechanism. The existence of a RAB7 compensatory mechanism is further displayed by the negligible changes to RAB5 in both inhibition models and CCZ1 in the siRAB7 model. While RAB5 and CCZ1 are upstream of RAB7 in the RAB7 cycle, they do not accumulate despite RAB7 inhibition. A lack of alteration in RAB5 and CCZ1 content between control and inhibitory groups does not mean that RAB7 inhibition has no impact on these proteins. For example, lack of RAB7(-GTP) may lead to a greater shift in the localization of RAB5 and CCZ1 to mitochondrial-enriched fractions. However, further research is needed. Despite the unexpected nature of these findings, they suggest that there is likely a compensatory mechanism when RAB7 is dysfunctional or deficient.

5.4 RAB7 is Required for C2C12 Differentiation and Myogenesis

To identify if RAB7 is critical for C2C12 differentiation and myogenesis, MYOG and MYH protein content and myotube morphology were analyzed in C2C12 cells that were treated with CID or knocked down *Rab7*. In both experiments there were no differences between the control and experimental groups in MYOG content. However, MYH was considerably lower at D3 and D5 in the CID group and at D2-D5 in the siRAB7 group when compared to their controls. To further investigate, immunofluorescent microscopy was used to identify morphological differences between experimental groups. Both experimental conditions had significantly lowered fusion and differentiation indices at D3 and D5 when compared to their controls. Moreover, the percentage of cells with 3 or more nuclei was also substantially lower in the CID and siRAB7 groups. Notably, knocking down *Rab7* results in drastically worse morphological outcomes, despite CID treated cells expressing less MYH protein. As aforementioned, differences in the specificity of CID and siRAB7 may account for this discrepancy. Since all RABs are critical for a variety of different cellular processes, having undesired inhibition of RABs other than RAB7 likely explain the differences between the two models. Thus, future experiments should determine the effect of CID on RAB7 activity in C2C12 cells to validate these findings. Regardless of specificity, cells treated with CID or siRAB7 were unhealthy. Many of these cells were not adherent to the cell culture plate by D5. This is one explanation for why there was less differentiation and myogenesis when RAB7 was inhibited. Further experiments should examine the impact of RAB7 inhibition on apoptosis to determine the fate of these non-adherent cells.

The only other study to link RAB7 to decreased myogenesis was conducted by Melendez, et al. (2021; 86). In this study, the researchers transfected RAB7-T22N (a constitutively inactive dominant negative) which abolishes RAB7 activity (86). Although it is a different experimental model, both CID and siRAB7 resulted in similar fusion index deficits. When considering Melendez, et al. (2021; 86)'s study and **Figures 6** and **9** of this thesis, it can be concluded that RAB7 is required for the progression of mammalian myoblast differentiation and myogenesis. Melendez, et al. (2021; 86) were able to link myoblast fusion deficits to RAB7's inability to facilitate degradation of TGFβs. Additionally, previous studies have emphasized the importance of autophagy in C2C12 differentiation (12,13,29,31,32). Thus, further investigation into the seemingly intimate connection between RAB7, autophagy, and C2C12 differentiation is required.

5.5 CID and siRAB7 Leads to Defects in Autophagy

To elucidate RAB7's importance in mediating autophagy during C2C12 differentiation, various autophagy markers were analyzed. There was drastically less SQSTM1 at D0, followed by a sustained decrease at D1 in the CID group, whereas the siRAB7 group had more content at D3 and D5. Additionally, there was more LC3-II content at D0, and D2-D5 in CID treated cells, and D2-D5 in siRAB7 cells compared to their controls. Generally, LC3-I content does not change in either RAB7 inhibition condition. LC3-II/LC3-I ratio is elevated as soon as differentiation is induced in siRAB7 cells, though this pattern did not apply to CID treated cells. This SQSTM1 and LC3 data highlights that autophagy is altered when RAB7 is inhibited. There are two hypotheses that can explain the phenomenon seen in LC3-II content: either autophagy is

upregulated or there is LC3-II accumulation when RAB7 is inhibited. As previous studies have observed (summarized by 37), when *Rab7* is knocked out there is an accumulation of enlarged LC3-II-positive autolysosomes in mammalian cells, thus it is logical that this is the case for C2C12 cells. The first result that supports this hypothesis is that CQ-induced flux experiments show that LC3-II and SQSTM1 are drastically lowered in CID treated cells compared to the CTRL. Although these findings were not found when comparing siRAB7 cells to the Scr, both CQ experiments still suggest that there is likely no RAB7-specific increase in autophagic flux. Flux experiments also found that CQ does not induce accumulation of RAB7 as seen in **Appendix A**. These flux experiments, in tandem with decreased ATG7, disrupted SQSTM1, and increased LC3-II provide evidence that there is likely an accumulation of autophagosomes and/or autolysosomes rather than an upregulation of autophagy when RAB7 is inhibited.

To determine if the UPS compensates for this RAB7-dependent autophagy deficit, proteasome activity was analyzed. It was hypothesized that the UPS would compensate for autophagic disruption as it is well known that ubiquitination of proteins and their subsequent binding to SQSTM1 mediate the crosstalk between autophagy and the UPS pathways (summarized by 30). Although mostly insignificant, there were dramatic decreases in proteasome activity at D0-D2 of both RAB7-inhibitory groups compared to their controls. These decreases in proteasome activity, in tandem with less SQSTM1 content at D0 and accumulating SQSTM1 at D3 and D5 in siRAB7 experiments, supports the hypothesis that autophagy, the UPS, and the crosstalk between them are likely dysfunctional in RAB7 inhibition experiments. This is likely the case as RAB7 is known to interact with and influence the localization and activity of PSMA7 (proteasomal alpha-subunit) and E3-Ub ligase (RNF115) (62-64). Although untested, E3-Ub

ligases other than RNF115 may also interact with RAB7 and be altered in RAB7 inhibition experiments, which would further supplement these findings.

Altogether, **Figures 7** and **10** provide evidence that RAB7 is critical for autophagy in differentiating C2C12 cells. Specifically, the data suggests that there is likely autophagosome and/or autolysosome accumulation, unaltered or decreased autophagic flux, and faulty crosstalk between the UPS and autophagy. This data provides an autophagic mechanism that explains why RAB7 inhibition results in decreased C2C12 differentiation and myogenesis. Future research should further investigate RAB7's role in pro-autophagy signaling and autophagosome biogenesis (specifically the interaction between BECN1 and RAB7), the crosstalk between autophagy and the UPS, ALR, and mitophagy in differentiating C2C12 cells.

Chapter 6: Study Summary and Other Considerations

6.1 Conclusion

Multiple studies have discovered an intimate connection between RAB7, autophagy, and mitophagy (10,12,13,29,31,32). Autophagy and mitophagy are also known to be critical for C2C12 differentiation and myogenesis. Despite this significance, no studies have investigated the complex interconnected relationship between RAB7, autophagy, and C2C12 differentiation until now. This thesis contains three novel findings. First, the RAB7 cycle is inherently connected to C2C12 differentiation. Second, RAB7 is required for myoblast differentiation and myogenesis. And third, RAB7-mediated differentiation deficits are likely caused by defective autophagy, the UPS, and the crosstalk between them. In accordance with existing literature (77-79,82), the high degree of mitochondrial-localized RAB7 during C2C12 differentiation suggests that RAB7 plays a role in mitochondrial dynamics, specifically mitophagy. However, further research is required. Overall, this thesis explains a novel critical role that RAB7 plays in mammalian myoblast differentiation and myogenesis.

6.2 Limitations

The data gathered through subcellular fractionation presents a limitation in this study. Nuclear fractions were not collected, and from the fractions that were collected, nuclear contamination was not tested by immunoblotting for Histone H2B. Currently, no studies have tested nuclear localization of RAB7 or other constituents of the RAB7 cycle, meaning nuclear contamination may skew mitochondrial and cytosolic fractionation patterns. Furthermore, the presence of RAB5, CCZ1, RAB7, and RABGDI, within nuclear fractions were also not quantified.

The next set of limitations focuses on RAB7-inhibitory experiments. First, as tested by Agola, J. O., et al. (2012), although CID1067700 is a nucleotide-binding competitive inhibitor that works against RAB7, many other GTP-binding proteins are also affected to a lesser degree (87). As aforementioned, CID at a concentration of 100nM decreases the activity of other GTP-binding proteins by up to 50% (87). This means that the results shown by CID are not specific to RAB7, but also affect other proteins, thus explaining differences seen between CID and siRAB7 experiments. Second, although siRNA transfection is a commonly used and widely accepted form of knocking down specific proteins, each transfection is variable in efficiency. Therefore, some of the observed differences between siRAB7 and Scr may be attributed to the transfection process, rather than the knockdown of *Rab7*. Last, due to the design of the CQ experiments, there is a high chance of variability when comparing between conditions. For example, since the CTRL and CID samples were loaded on separate gels, transferred onto separate membranes, and incubated with separate antibody vials, there is a sizeable chance that differences seen between groups are caused by experimental variability. To attempt to rectify this error, multiple standards were used per gel to try and normalize the samples properly within and between gels. The gels were transferred at the same time, with the same conditions, in the same transfer tray to reduce differences in protein transfer between gels. And finally, equal volumes of primary and secondary antibodies from the same vial were allocated to each membrane to ensure that there were minimal differences during antibody incubation. Even with these considerations, experimental errors likely occurred. For example, the loading control blot (GAPDH) in **Figure 10D** is not equal between membranes. In future experiments, the time-course should be shortened so that samples are loaded on one gel to allow for more accurate comparisons. This

experimental consideration along with differences in specificity between CID and siRAB7, may explain why the patterns seen in CQ experiments are different between experimental models.

6.3 Future Directions

Future researchers can pursue many meaningful directions in relation to RAB7 and mammalian skeletal muscle physiology. RAB7 may be important for autophagic signaling and autophagosome biogenesis, as seen with decreased autophagic flux in CID treated cells and ATG7 content. Quantification of Ad-RFP-GFP-LC3 fluorescence and co-localization through microscopy could confirm the accumulation of autophagosomes and/or autolysosomes during RAB7-inihbition experiments. Since the UPS does not compensate for autophagic deficits seen in RAB7-inhibition experiments, RAB7's role in mediating the UPS and its crosstalk with autophagy should be further explored. Ultimately, a more comprehensive examination of RAB7's role in autophagy can prove useful for researchers that want to target RAB7 as an autophagy regulator. In accordance with other publications (77-79,82), this thesis shows that RAB7 localizes to mitochondrial-enriched fractions, meaning that RAB7 likely participates in mitochondrial dynamics, specifically mitophagy. Because mitophagy is critical for C2C12 differentiation, research into possible defects in this pathway could provide more understanding of RAB7's importance in myoblast differentiation and myogenesis. Additionally, by D5 many cells were so unhealthy that they became non-adherent to the culture plate. Future studies should investigate to see if inhibiting RAB7 promotes apoptosis of these cells. Since the protein content of multiple constituents of the RAB7 cycle are largely unaltered when RAB7 is inhibited, investigation into potential compensatory mechanisms could elucidate an important target for

when RAB7 is faulty. RAB9 and RAB11 are strong compensatory contenders. The RAB9-depedent autophagy/mitophagy mechanism is independent of the canonical ATG7-mediated pathway (summarized by 33). Also, inhibition of RAB11 leads to increased myoblast fusion through blocking endocytic transport of TGFβs (86). RAB9 or RAB11 may compensate RAB7-mediated differentiation deficits by exploiting RAB7-independent autophagy, mitophagy, and/or endocytosis mechanisms. Finally, future studies should investigate the importance of RAB7 in skeletal muscle physiology *in-vivo*. It is well known that CMT2B is a peripheral neuropathy that results in muscle weakness (65). However, this thesis is the first study to show that RAB7 is required for mammalian myoblast differentiation and myogenesis. Thus, future studies should investigate if the differentiation deficits seen *in-vitro* can be replicated *in-vivo*, as well as RAB7's role at the muscle level in healthy, aging, and diseased muscle.

Bibliography

(1) Yin, H., Price, F., & Rudnicki, M. A. (2013) Satellite Cells and the Muscle Stem Cell Niche. *Physiol Rev. 93*(1):23-67. doi: 10.1152/physrev.00043.2011.

(2) Iwanami, S., & Iwami, S. (2019) Quantitative Immunology by Data Analysis Using Mathematical Models. *Encyclopedia of Bioinformatics and Computational Biology. 2*:984-987. doi: 10.1016/B978-0-12-809633-8.20250-1.

(3) Bentzinger, C. F., Wang, Y. X., & Rudnicki, M. A. (2012) Building Muscle: Molecular Regulation of Myogenesis. *Cold Spring Perspect Biol. 4*(2):a008342. doi: 10.1101/cshperspect.a008342.

(4) Schmidt, M., Schüler, S. C., Hüttner, S. S., & von Eyss, B. (2019) Adult stem cells at work: regenerating skeletal muscle. *Cell Mol Life Sci. 76*(13):2559-2570. doi:10.1007/s00018-019-03093-6.

(5) Kadi, F., et al. (2005) The behaviour of satellite cells in response to exercise: what have we learned from human studies? *Pflugers Arch. 451(2)*:319-327. doi: 10.1007/s00424-005-1406-6.

(6) Jiwlawat, N., Lynch, E., Jeffrey, J., Van Dyke, J. M., Suzuki, M. (2018) Current Progress and Challenges for Skeletal Muscle Differentiation from Human Pluripotent Stem Cells Using Transgene-Free Approaches. *Stem Cells Int.* 2018:6241681. doi: 10.1155/2018/6241681

(7) Kim, M., et al. (2015) The combination of ursolic acid and leucine potentiates the differentiation of C2C12 murine myoblasts through the mTOR signaling pathway. *Int J Mol Med. 35*(3):755-762. doi: 10.3892/ijmm.2014.2046.

(8) Hamai, N., Nakamura, M., & Asano, A. (1997) Inhibition of mitochondrial protein synthesis impaired C2C12 myoblast differentiation. *Cell Struct Funct. 22*(4):421-431. doi: 10.1247/csf.22.421.

(9) Devlin, R. B., & Emerson, C. P. Jr. (1978) Coordinate regulation of contractile protein synthesis during myoblast differentiation. *Cell. 13*(4):599-611. doi: 10.1016/0092-8674(78)90211-8

(10) Sin, J., et al. (2016) Mitophagy is required for mitochondrial biogenesis and myogenic differentiation of C2C12 myoblasts. *Autophagy. 12*(2):369-380. doi: 10.1080/15548627.2015.1115172.

(11) Bloemberg, D., & Quadrilatero, J. (2016) Autophagic flux data in differentiated C2C12 myotubes following exposure to acetylcholine and caffeine. *Data Brief.* 7:692-696. doi: 10.1016/j.dib.2016.03.008.

(12) McMillan, E. M., & Quadrilatero, J. (2014) Autophagy is required and protects against apoptosis during myoblast differentiation. *Biochem J. 462*(2):267-277. doi: 10.1042/BJ20140312.

(13) Baechler, B. L., Bloemberg, D., & Quadrilatero, J. (2019) Mitophagy regulates mitochondrial network signaling, oxidative stress, and apoptosis during myoblast differentiation. *Autophagy. 15*(9):1606-1619. doi: 10.1080/15548627.2019.1591672.

(14) Hansen, M., Rubinsztein, D. C., & Walker, D. W. (2018) Autophagy as a promoter of longevity: insights from model organisms. *Nat Rev Mol Cell Biol. 19*(9):579-593. doi: 10.1038/s41580-018-0033-y.

(15) Parzych, K. R. & Klionsky, D. J. (2014) An Overview of Autophagy: Morphology, Mechanism, and Regulation. *Antioxid Redox Signal. 10*(3):460-473. doi: 10.1089/ars.2013.5371.

(16) Byun, S., Lee, E., & Lee, K. W. (2017) Therapeutic Implications of Autophagy Inducers in Immunological Disorders, Infection, and Cancer. *Int J Mol Sci. 18*(9):1959. doi: 10.3390/ijms18091959.

(17) Filomeni, G., Zio, D., & Cecconi, F. (2014) Oxidative stress and autophagy: the clash between damage and metabolic needs. *Cell Death Differ. 22*(3):377-388. doi: 10.1038/cdd.2014.150.

(18) Galati, S., Boni, C., Gerra, M, Lazzaretti, M., & Bushini, A. (2019) Autophagy: A Player in response to Oxidative Stress and DNA Damage. *Oxid Med Cell Longev.* 2019:5692958. doi: 10.1155/2019/5692958.

(19) Marín-García, J. (2014) Chapter 14 - Oxidative Stress and Cell Death in Cardiovascular Disease: A Post-Genomic Appraisal. *Post-Genomic Cardiology.* (2nd ed.):471-498. Academic Press. doi: 10.1016/B978-0-12-404599-6.00014-7.

(20) Zhong, Y., et al. (2009) Distinct regulation of autophagic activity by Atg14L and Rubicon associated with Beclin 1-phosphatidylinositol-3-kinase complex. *Nat Cell Biol. 11(4)*:468-476. doi: 10.1038/ncb1854.

(21) Bjørkøy, G., Lamark, T., Pankiv, S., Øvervatn, A., Brach, S., & Johansen, T. Monitoring autophagic degradation of p62/SQSTM1. *Methods Enzymol.* 452:181-197. doi: 10.1016/S0076-6879(08)03612-4.

(22) Tanida, I., Ueno, T., & Kominami, E. LC3 and Autophagy. *Methods Mol Biol.* 445:77-88. doi: 10.1007/978-1-59745-157-4_4.

(23) Bento, C. F., Puri, C., Moreau, K., & Rubinsztein, D. C. (2013) The role of membrane-trafficking small GTPases in the regulation of autophagy. *J Cell Sci. 126*(Pt5):1059-1069. doi: 10.1242/jcs.123075.

(24) Saftig, P., Beertsen, W., & Eskelinen, E-L. (2008) LAMP-2: a control step for phagosome and autophagosome maturation. *Autophagy. 4*(4):510-512. doi: 10.4161/auto.5724.

(25) Eskelinen, E. L. (2006) Roles of LAMP-1 and LAMP-2 in lysosome biogenesis and autophagy. *Mol Aspects Med. 27*(5-6):495-502.

(26) Cooper, G. M. (2000) Lysosomes. *The Cell: A Molecular Approach. 2nd edition. Sinauer Associates.* NCBI ID: NBK9953.

(27) Lawrence, R. E., & Zoncu, R. (2019) The lysosome as a cellular centre for signalling, metabolism and quality control. *Nat Cell Biol. 21*(2):133-142. doi: 10.1038/s41556-018-0244-7.

(28) Chen, Y., & Yu, L. (2017) Recent progress in autophagic lysosome reformation. *Traffic. 18*(6):358-361. doi: 10.1111/tra.12484.

(29) Kuma, A., Komatsu, M., & Mizushima, N. (2017) Autophagy-monitoring and autophagy-deficient mice. *Autophagy. 13*(10):1619-1628. doi: 10.1080/15548627.2017.1343770.

(30) Kocaturk, N. M. & Gozuacik, D. (2018) Crosstalk Between Mammalian Autophagy and the Ubiquitin-Proteasome System. *Front Cell Dev Biol. 6*:128. doi: 10.3389/fcell.2018.00128.

(31) Xu, J., Cui, X., Wang, T. T., & Sachdev, U. (2015) Extended Treatment with Chloroquine, an Inhibitor of Autophagy, Disrupts Angiogenic Drive in Muscle after Arterial Ligation Without Detrimental Effects on Muscle Inflammation and Regeneration. *J Am Coll Surg. 221(4)*:S179. doi: 10.1016/j.jamcollsurg.2015.07.426.

(32) Sakane, H., & Akasaki, K. (2018) The Major Lysosomal Membrane Proteins LAMP-1 and LAMP-2 Participate in Differentiation of C2C12 Myoblasts. *Biol Pharm Bull. 41*(8):1186-1193. doi: 10.1248/bpb.b17-01030.

(33) Ao, X., Zou, L., & Wu, Y. (2014) Regulation of autophagy by the Rab GTPase network. *Cell Death Differ. 21*(3):348-358. doi: 10.1038/cdd.2013.187.

(34) Corbeel, L., & Freson, K. (2008) Rab proteins and Rab-associated proteins: major actors in the mechanism of protein-trafficking disorders. *Eur J Pediatr. 167*(7):723-729. doi: 10.1007/s00431-008-0740-z.

(35) Brighouse, A., Dacks, J. B., & Field, M. C. (2010) Rab protein evolution and the history of the eukaryotic endomembrane system. *Cell Mol Life Sci. 67*(20):3449-3465. doi: 10.1007/s00018-010-0436-1.

(36) Hoepflinger, M. C., Hametner, C., Ueda, T., & Foissner, I. (2014) Vesicular trafficking in characean green algae and the possible involvement of a VAMP72-family protein. *Plant Signal Behav. 9*(4):e28466. doi: 10.4161/psb.28466.

(37) Kuchitsu, Y., & Fukuda, M. (2018) Revisiting Rab7 Functions in Mammalian Autophagy: Rab7 Knockout Studies. *Cells. 7*(11):215. doi: 10.3390/cells7110215.

(38) Guerra, F., & Bucci, C. (2016) Multiple roles of the Small GTPase Rab7. *Cells. 5*(3):34. doi: 10.3390/cells5030034.

(39) Kawamura, N., et al. (2012) Delivery of endosomes to lysosomes via microautophagy in the visceral endoderm of mouse embryos. *Nat Commun. 3*:1071. doi: 10.1038/ncomms2069.

(40) Roy, S. G., Stevens, M. W., So, L., & Edinger, A. L. (2013) Reciprocal effects of rab7 deletion in activated and neglected T cells. *Autophagy. 9(7)*:1009-1023. doi: 10.4161/auto.24468.

(41) RAB7A member RAS oncogene family [Homo sapiens (human)]. (2020) *NCBI* – Gene. https://www.ncbi.nlm.nih.gov/gene/7879.

(42) RAB7B member RAS oncogene family [Homo sapiens (human)]. (2020) *NCBI* – Gene. https://www.ncbi.nlm.nih.gov/gene/338382.

(43) Stroupe, C. (2018) This Is the End: Regulation of Rab7 Nucleotide Binding in Endolysosomal Trafficking and Autophagy. *Front Cell Dev Biol. 6*:129. doi: 10.3389/fcell.2018.00129.

(44) Modica, G., & Lefrancois, S. (2020) Post-translational modifications: How to modulate Rab7 functions. *Small GTPases. 11(3)*:167-173. doi: 10.1080/21541248.2017.1387686.

(45) Mohapatra, G., et al. (2019) A SUMOylation-dependent switch of RAB7 governs intracellular life and pathogenesis of Salmonella Typhimurium. *132(1)*:jcs222612. doi: 10.1242/jcs.222612.

(46) Yamasaki, E. M., Molina, F. R., & Novick, P. (2013) GTPase Networks in Membrane Traffic. *Annu Rev Biochem. 81*:637-659. doi: 10.1146/annurev-biochem-052810-093700.

(47) Mottola, G. (2014) The complexity of Rab5 to Rab7 transition guarantees specificity of pathogen subversion mechanisms. *Front Cell Infect Microbiol. 4*:180. doi: 10.3389/fcimb.2014.00180.

(48) Ravikumar, B., Imarisio, S., Sarkar, S., O'Kane, C. J., & Rubinsztein, D. C. (2008) Rab5 modulates aggregation and toxicity of mutant huntingtin through macroautophagy in cell and fly models of Huntington disease. *J Cell Sci. 121(Pt 10)*:1649-1660. doi: 10.1242/jcs.025726.

(49) Yamaguchi, H., Nakagawa, I., Yamamoto, A., Amano, A., Noda, T., & Yoshimori, T. (2009). An initial step of GAS-containing autophagosome-like vacuoles formation requires Rab7. *PLoS Pathog (5)*11:e1000670. doi: 10.1371/journal.ppat.1000670.

(50) Yamano, K., et al. (2018) Endosomal Rab cycles regulate Parkin-mediated mitophagy. *Elife.* Pii:e31326. doi: 10.7554/eLife.31326.

(51) Yamano, K., Fogel, A. I., Wang, C., van der Bliek, A. M., & Youle, R. J. (2014) Mitochondrial Rab GAPs govern autophagosome biogenesis during mitophagy. *Elife. 3*: e01612. doi: 10.7554/eLife.01612.

(52) Bhargava, H., et al. (2020) Structural basis for autophagy inhibition by the human Rubicon-Rab7 complex. Proc Natl Acad Sci U S A. *117(29)*:17003-17010. doi: 10.1073/pnas.2008030117.

(53) Jaber, N., et al. (2016) Vps34 regulates Rab7 and late endocytic trafficking through recruitment of the GTPase-activating protein Armus. *J Cell Sci. 129(23)*:4424-4435. doi: 10.1242/jcs.192260.

(54) Harrison, R. E., Bucci, C., Vieira, O. V., Schroer, T. A., & Grinstein, S. (2003) Phagosomes Fuse with Late Endosomes and/or Lysosomes by Extension of Membrane Protrusions along Microtubules: Role of Rab7 and RILP. *Mol Cell Biol. 23(18)*:6494-6506. doi: 10.1128/MCB.23.18.6494-6506.2003.

(55) Zhao, Y. G. & Zhang, H. (2019) Autophagosome maturation: An epic journey from the ER to lysosomes. *J Cell Biol. 218(3)*:757-770. doi: 10.1083/jcb.201810099.

(56) Sun, Q., Westphal, W., Wong, K. N., Tan, I., & Zhong, Q. (2010) Rubicon controls endosome maturation as a Rab7 effector. *Proc Natl Acad Sci U S A. 107(45)*:19338-19343. doi: 10.1073/pnas.1010554107.

(57) Kuchitsu, Y., Homma, Y., Fujita, N., & Fukuda, M. (2018) Rab7 knockout unveils regulated autolysosome maturation induced by glutamine starvation. *J Cell Sci. 131(7)*:jcs215442. doi: 10.1242/jcs.215442.

(58) Yu, L., et al. (2010) Autophagy termination and lysosome reformation regulated by mTOR. *Nature. 265*(7300):942-946. doi: 10.1038/nature09076.

(59) Hyttinen, J. M., Niittykoski, M., Salminen, A., & Kaarniranta, K. (2013) Maturation of autophagosomes and endosomes: a key role for Rab7. *Biochem Biophys Acta. 1833*(3):503-510. doi: 10.1016/j.bbamcr.2012.11.018.

(60) Gutierrez, M. G., Munafó, D. B., Berón, W., & Colombo, M. I. (2004) Rab7 is required for the normal progression of the autophagic pathway in mammalian cells. *J Cell Sci. 117(Pt 13)*:2687-2897. doi: 10.1242/jcs.01114.

(61) Jäger, S., et al. (2004) Role for Rab7 in maturation of late autophagic vacuoles. *J Cell Sci. 117(Pt 20)*:4837-4848. doi: 10.1242/jcs.01370.

(62) Dong, J., Chen, W., Welford, A., & Wandinger-Ness, A. (2004) The proteasome α-Subunit XAPC7 Interacts Specifically with Rab7 and Late Endosomes. *J Biol Chem. 279(20)*:21334-21342. doi: 10.1074/jbc.M401022200.

(63) Sakane, A., Hatakeyama, S., & Sasaki, T. (2007) Involvement of Rabring7 in EGF receptor degradation as an E3 ligase. *Biochem Biophys Res Commun. 357(4)*:1058-1064. doi: 10.1016/j.bbrc.2007.04.052.

(64) Mizuno, K., Kitamura, A., & Sasaki, T. (2003) Rabring7, a Novel Rab7 Target Protein with a RING Finger Motif. *Mol Biol Cell. 14(9)*:3741-3752. doi: 10.1091/mbc.E02-08-0495.

(65) Colecchia, D., et al. (2018) Alterations of autophagy in the peripheral neuropathy Charcot-Marie-Tooth type 2B. *Autophagy. 14(6):*930-941. doi: 10.1080/15548627.2017.1388475.

(66) Tilokani, L., Nagashima, S., Paupe, V., & Prudent, J. (2018) Mitochondrial dynamics: overview of molecular mechanisms. *Essays Biochem. 62*(3):341-360. doi: 10.1042/EBC20170104.

(67) Seo, A. Y., Joseph, S. M., Dutta, D., Hwang, J. C., Aris, J. P., & Leeuwenburgh, C. (2010) New insights into the role of mitochondria in aging: mitochondrial dynamics and more. *J Cell Sci. 123*(Pt 15):2533-2542. doi: 10.1242/jcs.070490.

(68) Palikaras, K., Lionaki, E., & Tavernarakis, N. (2015) Balancing mitochondrial biogenesis and mitophagy to maintain energy metabolism homeostasis. *Cell Death Differ. 22*(9):1399-1401. doi: 10.1038/cdd.2015.86.

(69) Zorova, L. D., et al. (2018) Mitochondrial membrane potential. *Anal Biochem.* 552:50-59. doi: 10.1016/j.ab.2017.07.009.

(70) Herst, P. M., Roew, M. R., Carson, G. M., & Beeridge, M. V. (2017) Functional Mitochondria in Health and Disease. *Front Endocrinol (Lausanne)*. 8:296. doi: 10.3389/fendo.2017.00296.

(71) Jin, S. M., & Youle, R. J. (2012) PINK1- and Parkin-mediated mitophagy at a glance. *J Cell Sci. 125*(Pt 4):795-799. doi: 10.1242/jcs.093849.

(72) Durcan, T. M., & Fon, E. A. (2015) The three 'P's of mitophagy: PARKIN, PINK1, and post-translational modifications. *Genes Dev. 29*(10):989-999. doi: 10.1101/gad.262758.115.

(73) Von Stockum, S., Marchesan, E., & Ziviani, E. (2018) Mitochondrial quality control beyond PINK1/Parkin. *Oncotarget. 9*(16):12550-12551. doi:10.18632/oncotarget.23799

(74) Villa, E., Marchetti, S., & Ricci, J. E. (2018) No Parkin Zone: Mitophagy without Parkin. *Trends Cell Biol. 28*(11):882-895. doi: 10.1016/j.tcb.2018.07.004.

(75) Yin, J., Puri, R., Yang, H., Lizzio, M. A., Wu, C., Sheng, Z., & Guo, M. (2014) MUL1 acts in parallel to the PINK1/parkin pathway in regulating mitofusin and compensates for loss of PINK1/parkin. *eLife. 3*:e01958. doi: 10.7554/eLife.01958.

(76) Yamada, T., Dawson, T. M., Yanagawa, T., Iijima, M., & Sesaki, H. (2019) SQSTM1/p62 promotes mitochondrial ubiquitination independently of PINK1 and PRKN/parkin in mitophagy. *Autophagy. 15*(11):2012-2018. doi: 10.1080/15548627.2019.1643185.

(77) Yamano, K., et al. (2018) Endosomal Rab cycles regulate Parkin-mediated mitophagy. *Elife.* Pii:e31326. doi: 10.7554/eLife.31326.

(78) Heo, J. M., Ordureau, A., Swarup, S., Paulo, J. A., Shen, K., Sabatinin, D. M., & Harper, J. W. (2018) RAB7A phosphorylation by TBK1 promotes mitophagy via the PINK-PARKIN pathway. *Sci Adv. 4*(11):eaav0443. doi: 10.1126/sciadv.aav0443.

(79) Yamano, K., Fogel, A. I., Wang, C., van der Bliek, A. M., & Youle, R. J. (2014) Mitochondrial Rab GAPs govern autophagosome biogenesis during mitophagy. *Elife. 3*:e01612. doi: 10.7554/eLife.01612.

(80) Wong, Y. C., Ysselstein, D., & Krainc, D. (2018) Mitochondria–lysosome contacts regulate mitochondrial fission via RAB7 GTP hydrolysis. *Nature. 554*(7692):382-386. doi: 10.1038/nature25486.

(81) Hollville, E., Carroll, R. G., Cullen, S. P., & Martin, S. J. (2014) Bcl-2 Family Proteins Participate in Mitochondrial Quality Control by Regulating Parkin/PINK1-Dependent Mitophagy. *Mol Cell. 55(3)*:451-466. doi: 10.1016/j.molcel.2014.06.001.

(82) Hammerling, B. C., Shires, S. E., Leon, L. J., Cortez, M. Q., & Gustafsson, Å, B. (2017) Isolation of Rab5-positive endosomes reveals a new mitochondrial degradation pathway utilized by BNIP3 and Parkin. *Small GTPases. 11*:1-8. doi: 10.1080/21541248.2017.1342749.

(83) Xian, H., Yang, Q., Xiao, L., Shen, H., & Liou, Y. (2019) STX17 dynamically regulated by Fis1 induces mitophagy via hierarchical macroautophagic mechanism. *Nat Commun. 10*(1):2059. doi: 10.1038/s41467-019-10096-1.

(84) Nakamura, K., Yamanouchi, K., & Nishihara, M. (2014) Secreted protein acidic and rich in cysteine internalization and its age-related alterations in skeletal muscle progenitor cells. *Aging Cell. 13(1)*:175-184. doi: 10.1111/acel.12168.

(85) Fujita, N., et al. (2017) Genetic screen in Drosophila muscle identifies autophagy-mediated T-tubule remodeling and a Rab2 role in autophagy. *eLife (6)*:e23367. doi: 10.7554/eLife.23367.

(86) Melendez, J., et al. (2021) TGFβ signalling acts as a molecular brake of myoblast fusion. *Nat Commun. 12(1)*:749. doi: 10.1038/s41467-020-20290-1.

(87) Agola, J. O., et al. (2012) A Competitive Nucleotide Binding Inhibitor: In vitro Characterization of Rab7 GTPase Inhibition. *ACS Chem Biol. 7(6)*:1095-1108. doi: 10.1021/cb3001099.

Appendix A

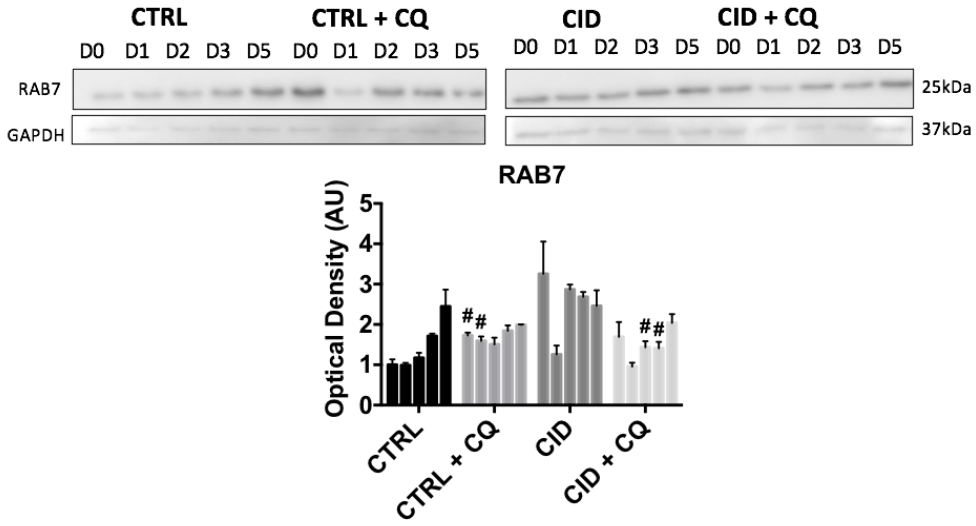

Supplementary Figure 1 – RAB7 Protein Content in CID CQ Experiments

CQ-induced flux experiments do not see a dramatic change in RAB7 content in vehicle control (CTRL) or CID treated cells. [n=4 independent experiments, mean ± SEM]

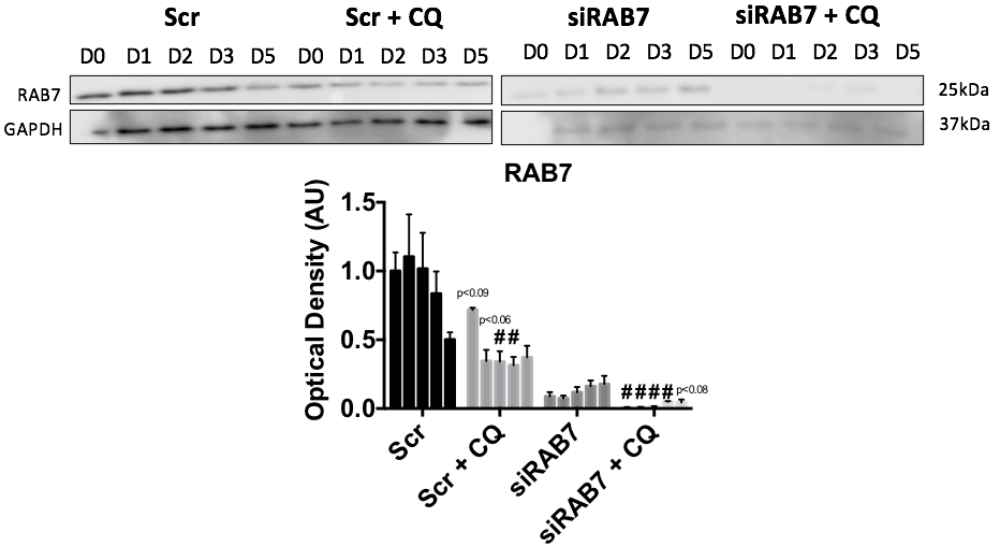

Supplementary Figure 2 – RAB7 Protein Content in siRAB7 CQ Experiments

CQ-induced flux experiments do not see a dramatic change in RAB7 content in scramble control (Scr) or siRAB7 cells. Furthermore, *Rab7* knockdown is shown between Scr and siRAB7. [n=4 independent experiments, mean ± SEM]